*Chapter Two*

# The Influence of Macrocyclic Polyether Constitution upon Ammonium Ion Binding

*"One ring to rule them all, One ring to find them,*
*One ring to bring them all and in the darkness bind them"*
J R R Tolkien

The research described in this **Chapter** is based upon four publications:

Ashton, P. R.; Bartsch, R. A.; **Cantrill, S. J.**; Hanes, Jr., R. E.; Hickingbottom, S. K.; Lowe, J. N.; Preece, J. A.; Stoddart, J. F.; Talanov, V. S.; Wang, Z.-H. *Tetrahedron Lett*. **1999**, *40*, 3661–3664.

Ashton, P. R.; **Cantrill, S. J.**; Preece, J. A.; Stoddart, J. F.; Wang, Z.-H.; White, A. J. P.; Williams, D. J. *Org. Lett.* **1999**, *1*, 1917–1920.

**Cantrill, S. J.**; Fulton, D. A.; Heiss, A. M.; Pease, A. R.; Stoddart, J. F.; White, A. J. P.; Williams, D. J. *Chem. Eur. J.* **2000**, *6*, 2274–2287.

**Cantrill, S. J.**; Preece, J. A.; Stoddart, J. F.; Wang, Z.-H.; White, A. J. P.; Williams, D. J. *Tetrahedron* **2000**, *56*, 6675–6681.

# Table of Contents

**Abstract:** A range of crown ethers with either [24]crown-8 or [25]crown-8 constitutions have been demonstrated to form pseudorotaxanes with *para*-disubstituted dibenzylammonium ions, in solution, the 'gas phase' and the solid state, by $^1$H NMR spectroscopy, liquid secondary ion mass spectrometry, and X-ray crystallography, respectively. Substitution of the [24]crown-8 framework with increasing numbers of benzo rings is observed to lower the stability constants ($K_a$'s) from $>10^3$ to ~0 $M^{-1}$ in acetonitrile. A pronounced decrease in $K_a$ values also occurs when the [24]crown-8 constitution is expanded to give a macroring containing 25 atoms – a modification that not only increases the size of the macrocyclic cavity, but also disrupts the O–C–C–O repeating unit in the macrocycle's backbone. In contrast with the other macrocycles, when tetrabenzo[24]crown-8 (TB24C8) is mixed with dibenzylammonium hexafluorophosphate (**7**·$PF_6$) in non-competitive solvents, the thermodynamically-driven noncovalent synthesis of the threaded 1:1 complex does not occur. However, on crystallization from solution—in a process that is presumably kinetically-controlled—TB24C8 molecules and $\mathbf{7}^+$ cations form an array of [2]pseudorotaxanes stabilized by a plethora of [C–H···F] hydrogen bonds to highly-ordered, interstitially-located $PF_6^-$ anions.

## 2.1. Introduction

The serendipitous discovery of crown ethers by Pedersen[1] just over thirty years ago is arguably the origin of many aspects of supramolecular chemistry[2] as we know it today. Although not the first to synthesize macrocyclic polyethers, it was Pedersen who realized their importance in the context of host-guest chemistry, and went on[3] to investigate the binding properties of crown ether hosts with a wide variety of cationic guests. Among the many guests studied[4,5] in later years were the ammonium ($NH_4^+$) and primary alkylammonium ($RNH_3^+$) ions, which were shown[6]—by Cram and others—to bind (Figure 2.1) dibenzo[18]crown-6 in a *face-to-face* manner. The binding of secondary dialkylammonium ions ($R_2NH_2^+$) was largely unexplored[7] until recent times, whereupon it was discovered[8] that, if a [24]crown-8-containing macrocyclic polyether is employed, the $R_2NH_2^+$ ion can interpenetrate fully (Figure 2.2) the

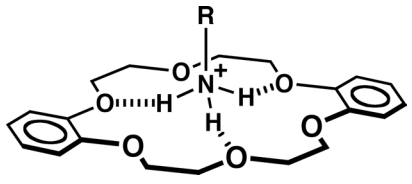


**Figure 2.1**. The *face-to-face* interaction between DB18C6 and a primary ammonium ion.

macrocyclic cavity, generating a so-called pseudorotaxane in which the cation is *threaded* through the center of the crown ether. This breakthrough heralded the arrival of a new paradigm for the construction of (1) discrete interlocked molecules,[9] and (2) extended interwoven supramolecular arrays.[10] For complexes exhibiting 1:1 stoichiometries, only dibenzo[24]crown-8 (**3**) (DB24C8) has been studied in detail, revealing that the self-assembly[11] of the [2]pseudorotaxane proceeds with the formation of both $N^+$–H···O and C–H···O hydrogen bonds, augmented by electrostatic and aromatic–aromatic interactions. More recently, it has been demonstrated[12] that the judicious substitution of the phenyl rings of the dibenzylammonium ions allows for the 'fine-tuning' of this supramolecular system. Indeed, a linear free energy relationship exists between the stability constants ($K_a$'s) for the formation of the pseudorotaxanes and the Hammett substituent constants ($\sigma$). This Chapter describes how changing the crown ether host, as opposed to the thread-like guest, alters the $K_a$'s for pseudorotaxane formation.

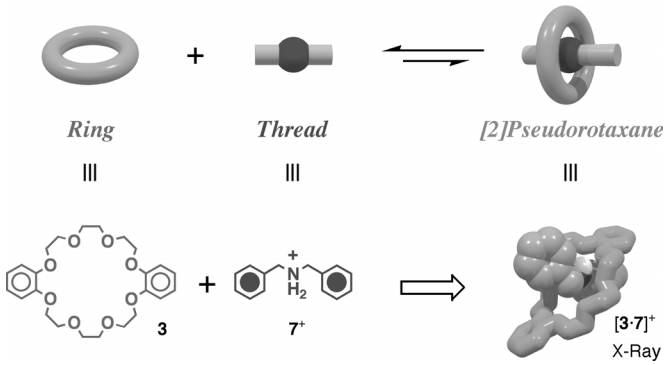


**Figure 2.2**. Top: A schematic representation depicting the formation of a threaded 1:1 complex (a ***Pseudorotaxane***) formed between two complementary species, whereupon the cavity of a suitably-sized ***Ring***-shaped component is skewered by a linear ***Thread***-like one. Bottom: A specific example of this concept showing how the dibenzylammonium cation $\mathbf{7}^+$ threads through DB24C8 (**3**).

## 2.2. Synthesis

The crown ethers (Chart 2.1) chosen for this investigation included [24]crown-8 (**1**) (24C8)[13] and three known derivatives with one, two, and four fused benzo-rings –

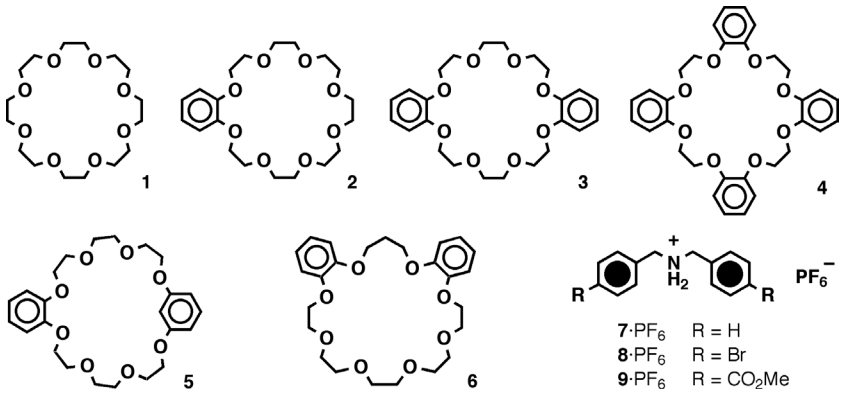


**Chart 2.1.**

namely benzo[24]crown-8 (**2**) (B24C8),[14] DB24C8 (**3**),[15] and tetrabenzo[24]crown-8 (**4**) (TB24C8),[16] respectively. Two macrocycles (**5** and **6**) with a [25]crown-8 constitution were also investigated. Dibenzo[24]crown-8 (**3**) is available commercially, and the other three [24]crown-8-based macrocycles under investigation were prepared according to literature procedures[13,16] or modifications thereof.[14] The synthetic pathway leading to the formation of benzometaphenylene[25]crown-8 (**5**) (BMP25C8) is depicted in Scheme 2.1. Tosylation of the diol[17] **10**, under standard conditions, afforded the ditosylate **11**.

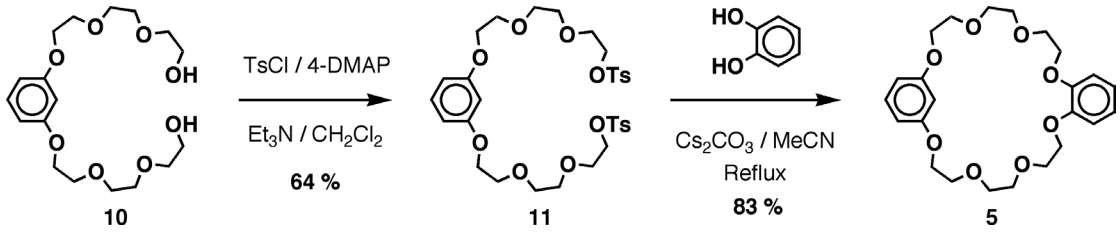


**Scheme 2.1**. The sythesis of BMP25C8 (**5**).

Subsequent macrocyclization of **11** with catechol, in the presence of base, gave the crown ether in good yield. A sample of the [25]crown-8-based macrocycle **6**, was provided[18] by the Bartsch group at Texas Tech University. The dibenzylammonium salts **7**·$PF_6$ and **8**·$PF_6$ were prepared according to literature procedures.[8b,12] The diester **9**·$PF_6$ was

prepared simply from the corresponding amine[9b] upon protonation (HCl / $H_2O$) and anion exchange ($NH_4PF_6$ / $H_2O$).

## 2.3. Mass Spectrometric Studies

It is evident (Table 2.1) that all of the crown ether hosts—*i.e.*, **1**–**6**—form 1:1 complexes with each of the secondary dibenzylammonium ion guests—*i.e.*, $\mathbf{7}^+$–$\mathbf{9}^+$—in the 'gas phase', as demonstrated by liquid secondary ion mass spectrometry (LSIMS). In each

**Table 2.1**. Relative intensities of complexed and uncomplexed species in the 'gas phase' as determined by LSIMS.[(a)]

| Guest | Observed Species | Relative Intensities of Mass Peaks (%) | | | | | |
|---|---|---|---|---|---|---|---|
| | | [24]Crown-8 ring | | | | [25]Crown-8 ring | |
| | | **1** | **2** | **3** | **4** | **5** | **6** |
| **7**·$PF_6$ | Free Guest ($\mathbf{7}^+$) | 47 | 48 | 46 | 175 | 200 | 141 |
| (R = H) | Free Crown (**1**–**6**) | 40 | 11 | 7 | 33 | 6 | 7 |
| | 1:1 Complex | 100 | 100 | 100 | 100[(b)] | 100[(b)] | 100[(b)] |
| **8**·$PF_6$ | Free Guest ($\mathbf{8}^+$) | 24 | 30 | 30 | 53 | 115 | 55 |
| (R = Br) | Free Crown (**1**–**6**) | 10 | 18 | 22 | 96 | 12 | 17 |
| | 1:1 Complex | 100 | 100 | 100 | 100 | 100[(b)] | 100 |
| **9**·$PF_6$ | Free Guest ($\mathbf{9}^+$) | 28 | 37 | 29 | 51 | 68 | 44 |
| (R = $CO_2Me$) | Free Crown (**1**–**6**) | 13 | 20 | 10 | 37 | 4 | 8 |
| | 1:1 Complex | 100 | 100 | 100 | 100 | 100 | 100 |

(*a*) The spectra were obtained on a VG Zabspec mass spectrometer, equipped with a cesium ion source and utilizing a *m*-nitrobenzyl alcohol matrix. (*b*) These values were scaled to 100 to aid comparisons between systems.

case, analysis of an MeCN solution[19] containing equimolar quantities of crown ether and dibenzylammonium salt, afforded a spectrum in which peaks were observed for (1) the crown ether adduct with $Na^+$, (2) the uncomplexed dibenzylammonium cation, and (3) the

1:1 complex formed between host and guest. For example, the LSI mass spectrum (Figure 2.3) obtained from an MeCN solution containing an equimolar mixture of DB24C8 (**3**) and **9**·$PF_6$ shows three such peaks, at *m/z* values of 417, 314, and 762, respectively. Although a peak corresponding to a 1:1 complex does not necessarily infer pseudorotaxane formation, the relatively high intensities recorded in Table 2.1 for all these species suggest very strongly[20] that they are indeed pseudorotaxanes and not just face-to-face complexes. Furthermore, it should be noted that the signals arising from complexes involving crown ethers **4**–**6** are much less intense than those for **1**–**3**. Although these mass spectrometric studies are by no means quantitative, this observation implies that TB24C8 (**4**) and the two [25]crown-8 macrocycles (**5** and **6**) bind dibenzylammonium ions less strongly than do the crown ethers **1**–**3**.

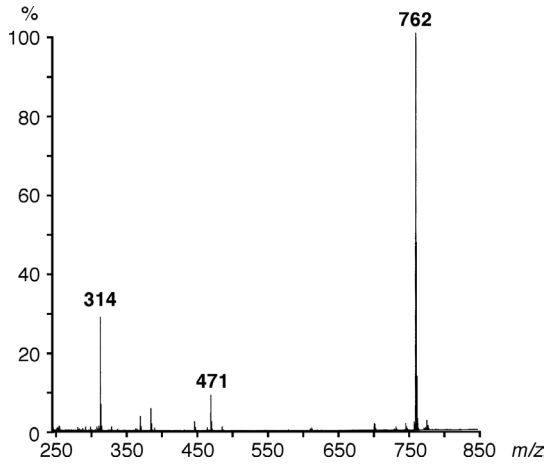


**Figure 2.3**. The LSI-mass spectrum of a 1:1 mixture of DB24C8 (**3**) and **9**·$PF_6$.

## 2.4. Solution Phase Studies

Each crown ether was mixed with an equimolar amount of the appropriate dibenzylammonium salt and their $^1$H NMR spectra (400 MHz, $CD_3CN$ or $(CD_3)_2CO$, 300 K) were recorded. In most cases, three different sets of resonances were observed, which could be assigned to (1) the free crown ether host, (2) the uncomplexed guest, and

(3) the 1:1 complex formed between the host and guest. This spectroscopic behavior indicates that the complexed and uncomplexed species are equilibrating slowly on the $^1$H NMR timescale, allowing $K_a$ values (Table 2.2) to be calculated utilizing the so-called single-point[21] method.

**Table 2.2**. The stability constants ($K_a$'s) calculated for the formation of pseudorotaxanes incorporating crown ethers **1**–**3**, **5** and **6** with guests **7**–**9**·$PF_6$.

| Guest | R | $K_a$ ($M^{-1}$) {300 K, 10 mM, $CD_3CN$} | | | | | |
|---|---|---|---|---|---|---|---|
| | | [24]Crown-8 ring | | | | [25]Crown-8 ring | |
| | | **1** | **2** | **3** | **4**(*a*) | **5** | **6** |
| **7**·$PF_6$ | H | 1700 | 470 | 320 | ~0(*b*) | —(*c*) | —(*c*) |
| **8**·$PF_6$ | Br | 3500 | 720 | 800 | ~0 | —(*c*) | —(*c*) |
| **9**·$PF_6$ | $CO_2Me$ | 4500 | 880 | 1100 | ~0 | ~50(*d*) | 270 |

(*a*) Measurements made on TB24C8 (**4**) were conducted at 5 mM in $CD_3COCD_3$. (*b*) Although no binding can be detected in solution by this method, this host/guest system has been shown (*vide infra*) to co-crystallize to give the [2]pseudorotaxane. (*c*) In these cases, the spectra consist of broadened peaks, indicating that the complexed and uncomplexed species are not equilibrating slowly enough on the $^1$H NMR timescale to use the single-point method to determine $K_a$ values. (*d*) Since the complexed and uncomplexed species are not equilibrating slowly on the $^1$H NMR timescale at 300 K, the stability constant was determined at lower temperatures (243–288 K) where the equilibration is slow and those values were used to extrapolate to an approximate room temperature value for $K_a$.

### *2.4.1. [24]Crown-8-Based Macrocycles*

With the exception of **4**, all of the [24]crown-8-based macrocycles formed complexes with each of the three dibenzylammonium ions (**7**$^+$–**9**$^+$) in solution. In each case, a spectrum containing distinct peaks—corresponding to both complexed and uncomplexed species—was observed, indicating (*vide supra*) that slow exchange kinetics are in operation, thus permitting a single-point determination of $K_a$. This phenomenon is best

exemplified in the $^1$H NMR spectrum (Figure 2.4) of a $CD_3CN$ solution containing an equimolar mixture of DB24C8 (**3**) and **9**·$PF_6$. In this spectrum, there are two AA'BB' systems arising from the *para*-disubstituted aromatic rings of $\mathbf{9}^+$, one corresponding to the bound species, and the other to the 'free' cation. This doubling up of signals—for both the cation and the crown ether—is observed throughout the spectrum, most notably

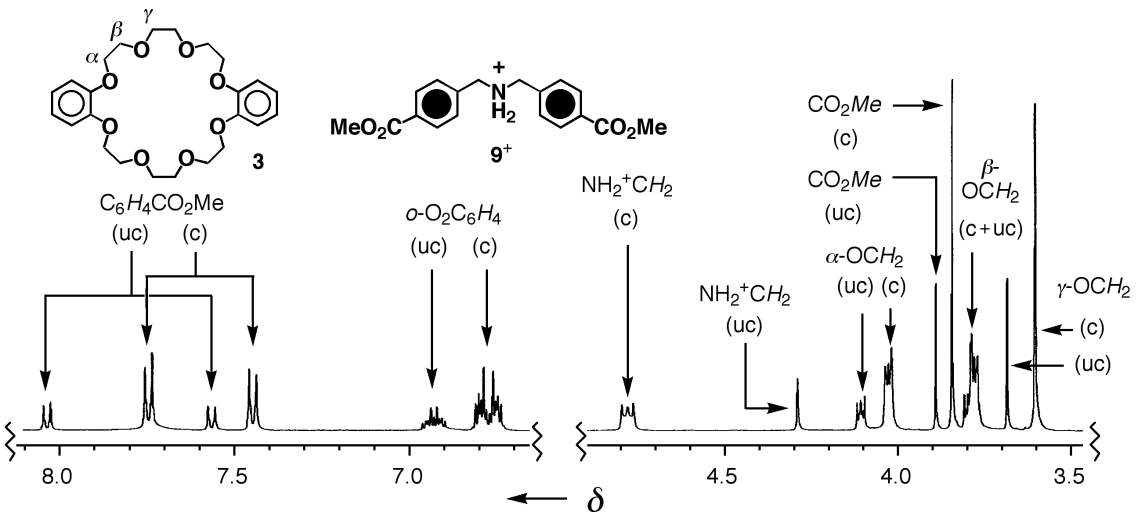


**Figure 2.4**. Partial $^1$H NMR spectrum (400 MHz, $CD_3CN$, 300 K), of an equimolar solution of DB24C8 (**3**) and **9**·$PF_6$ (both 10 mM), demonstrating that complexed (c) and uncomplexed (uc) species are equilibrating with one another slowly on the $^1$H NMR timescale.

for the methylene protons adjacent to the $NH_2^+$ center. Upon threading of the cation through the crown ether, the signal corresponding to the $CH_2$ group of the dibenzylammonium ion not only moves considerably downfield ($\Delta\delta \sim 0.5$ ppm), but also appears as a complex multiplet – rather than the singlet observed for these protons in the unbound cation. This highly characteristic change in multiplicity—arising as a consequence of coupling to the now slower-exchanging $NH_2^+$ protons—is highly diagnostic,[22] indicating that the crown ether is indeed encircling the $NH_2^+$ center.

Although investigations on the binding characteristics of TB24C8 (**4**) with dibenzylammonium salts were hampered by its low solubility in $CD_3CN$, it was sufficiently soluble in $CD_3COCD_3$[23] to permit binding measurements to be performed at 5 mM. Inspection of the resulting spectra of equimolar mixtures of this crown ether with the dibenzylammonium salts **7**–**9**·$PF_6$ revealed that there are negligible chemical shift changes under these conditions and so the $K_a$ values can, therefore, be assumed to be effectively zero.

### *2.4.2. [25]Crown-8-Based Macrocycles*

The $^1H$ NMR spectrum of a $CD_3CN$ solution containing equimolar quantities of BMP25C8 and **7**·$PF_6$ reveals the occurrence of complexation. However, the spectrum consists of both broad and sharp peaks—rather than a series of sharp, well-defined peaks arising from the slow exchange of the free components and the [2]pseudorotaxane (as is the case with the [24]crown-8 analogues **1**–**3**)—indicating that, under the experimental conditions, neither a slow- nor fast-exchange regime is operating. This behavior precludes the determination of a stability constant by either the single-point method[21] or dilution/titration[24] techniques.

At ambient temperature, the terminal Br and $CO_2Me$ groups of **8**·$PF_6$ and **9**·$PF_6$, respectively, did not provide enough extra steric bulk to slow down significantly the rate of exchange between complexed and uncomplexed species, and similarly broad spectra were observed. However, sharp signals were observed in the $^1H$ NMR spectra of a 1:1

mixture of **5** and **9**·$PF_6$ in $CD_3CN$ solution (Figure 2.5) recorded at 243, 258, 273, and 288 K, respectively. At these temperatures, equilibration between the [2]pseudorotaxane [**5**·**9**]$PF_6$ and its free components is slow on the $^1$H NMR timescale, allowing single-point determinations of $K_a$ values at each one of these temperatures. Subsequently, extrapolation of the van't Hoff plot (Figure 2.6) obtained using these data gives a value for $K_a$ at 300 K of ~50 $M^{-1}$.

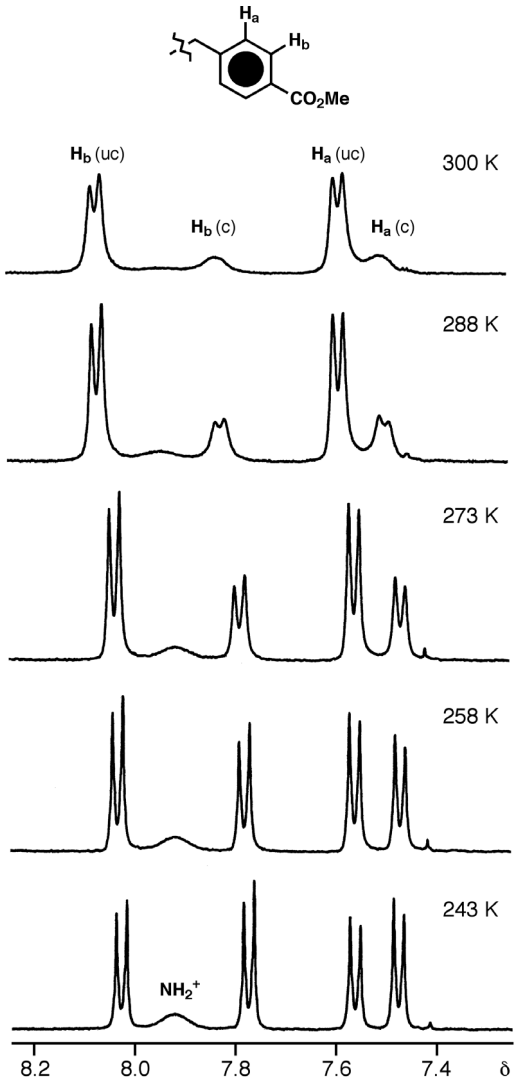


**Figure 2.5**. Partial $^1$H NMR spectra (the AA'BB' region) of a 1:1 mixture of BMP25C8 (**5**) and **9**·$PF_6$ in $CD_3CN$ solution over the temperature range 243–300 K.

The $^1$H NMR spectra obtained from mixtures of either **7**·$PF_6$ or **8**·$PF_6$, with the [25]crown-8-based macrocycle **6**, also contained broad peaks, indicating an intermediate rate of exchange—with respect to the $^1$H NMR timescale—between complexed and uncomplexed species. However, when its ability to bind **9**·$PF_6$ was investigated, a $^1$H NMR spectrum containing sharp peaks was obtained, indicating that a slow exchange regime was in operation. In this case, the methoxycarbonyl groups of $\mathbf{9}^+$ were sufficiently bulky to

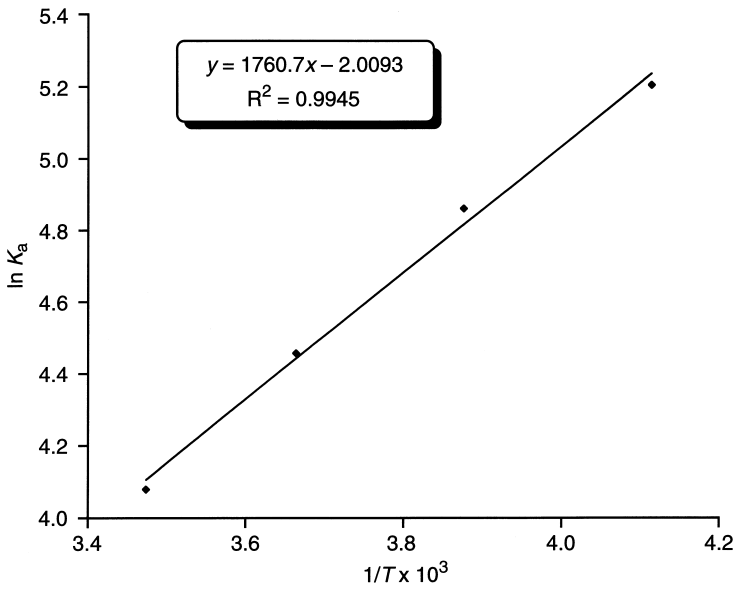


**Figure 2.6**. The van't Hoff plot obtained upon plotting ln $K_a$ *vs* $1/T$ for the $K_a$ values determined—using the single point method—over the temperature range 243–288 K.

slow the passage of **6** over them, enabling the value of $K_a$ for this process (270 $M^{-1}$) to be determined using the single-point method.

### *2.4.3. Summary of Solution Phase Studies*

As expected,[12] for the crown ethers **1**–**3**, the stability constants increase as the π-electron densities on the aromatic rings of the dibenzylammonium ion decrease, *i.e.*, on going from R = H to Br to $CO_2Me$, the $K_a$ values become larger. A comparison of how each crown ether host binds to any one particular guest, shows that, in the case of the [24]crown-8 constitution (**1**–**4**), the $K_a$ values decrease[25] as more of the macroring oxygen atoms 'become' phenolic. This observation can be rationalized in terms of the reduced basicity of these atoms—with respect to dialkyl ether oxygen atoms—and, as such, their effectiveness as hydrogen bond acceptors is diminished. The crown ethers with

[25]crown-8 constitutions (**5** and **6**) presumably have larger cavities than their [24]crown-8 counterparts, as evidenced by the increase in the rate of exchange between complexed and uncomplexed species when we consider the binding of either **7**·$PF_6$ or **8**·$PF_6$. These [25]crown-8 macrocyclic polyethers also contain structural elements that deviate from the ideal[4d] O–C–C–O repeating unit—there is a propyleneoxy moiety in **5** and a 1,3-phenylenedioxy moiety in **6**—disrupting the array of donor atoms directed toward the center of the crown ether cavity. This distortion seemingly results in a less-favorable geometry for interaction with the dibenzylammonium cation, hence giving rise to lower $K_a$ values in comparison to the 24-atom-containing macrorings, *cf.* the binding of **9**·$PF_6$ with crown ethers **1**–**3** as compared with **5** and **6**.

## 2.5. X-Ray Crystallographic Investigations

### *2.5.1. Background*

X-Ray crystallographic analysis has proven[26] to be an invaluable tool in the charaterization of crown ether/secondary dialkylammonium ion complexes. Since the first superstructure in this series—that of [**3**·**7**]$PF_6$ (Figure 2.7)—was analyzed,[8a] many more beautiful examples of solid-state superstructures formed from these building blocks—many of which are highlighted in Chapter 1—have been uncovered. To further the study of how crown ether constitution affects secondary

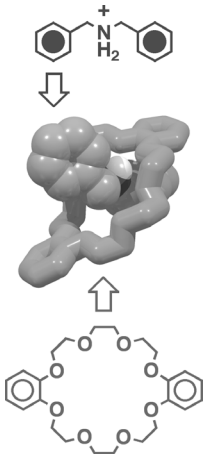

**Figure 2.7**. The X-ray crystal superstructure of [**3**·**7**]$PF_6$.

ammonium ion binding, attempts were made to crystallize previously unexplored[27] combinations of the crown ethers and dibenzylammonium salts under investigation in this Chapter.

### *2.5.2. Tetrabenzo[24]crown-8 (TB24C8)*

Although TB24C8 (**4**) has been shown to have a negligible affinity for the $\mathbf{7}^{+}$ cation in solution, the kinetically controlled crystallization of these two components affords a [2]pseudorotaxane array in the solid state. Single crystals of [**4**·**7**]$PF_6$ were obtained upon slow evaporation of a $CHCl_3$/MeCN/*n*-$C_6H_{14}$ (7:3:3) solution containing a 1:1 mixture of the 'thread' and 'ring' components. The X-ray crystallographic analysis reveals that the asymmetric unit contains *four* independent 1:1 complexes, each possessing (Figure 2.8) a very similar co-conformation,[28] with the only significant

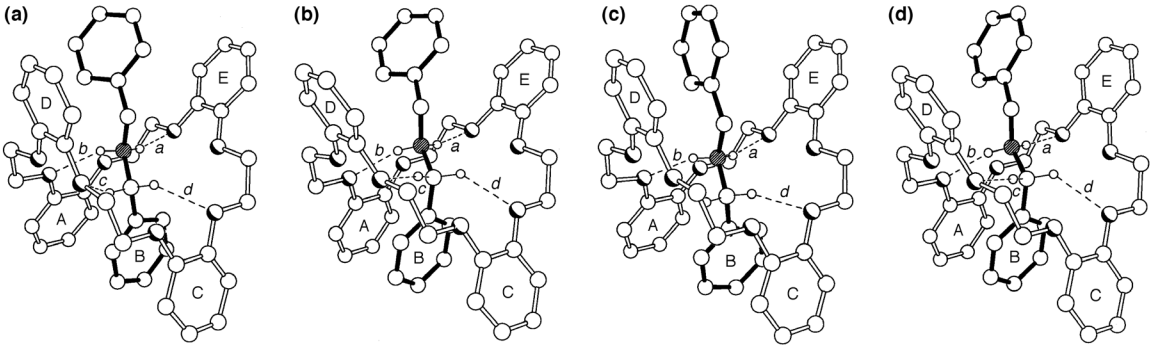


**Figure 2.8**. Ball-and-stick representations of the four crystallographically independent [2]pseudorotaxanes present in the crystals of [**4**·**7**]$PF_6$ showing the $N^{+}$–H···O and C–H···O hydrogen bonding. The hydrogen bonding geometries and inter-ring separations are given in Table 2.3.

difference being in the relative orientation of one of the benzyl groups with respect to the plane of the $C_{Ph}CH_2NH_2^{+}CH_2C_{Ph}$ backbone. The approximate tennis-ball-seam-

symmetry ($D_{2d}$) adopted by the TB24C8 macrocycle is similar to that observed (*vide infra*) in TB24C8·2MeCN. Stabilization of the individual 1:1 complexes is achieved (Table 2.3) *via* the usual combination of $N^+$–H···O (*a* and *b*) and C–H···O (*c* and *d*) hydrogen bonding interactions, which are supplemented by face-to-face $\pi$–$\pi$ stacking interactions whereby benzo rings A and C of the crown ether sandwich phenyl ring B of the $\mathbf{7}^+$ cation. These supermolecules are in turn stabilized by a wealth of C–H···F hydrogen bonding[29] interactions (Table 2.4) originating from a highly ordered matrix formed by the associated $PF_6^-$ anions. The unusual lack of disorder observed for the $PF_6^-$ anions is perhaps indicative of their participation[30] in directing the formation of the overall three-dimensional lattice. The $PF_6^-$ anions are embedded (Figure 2.9) into layers of the 1:1 complexes, occupying clefts (Figure 2.10) formed between each group of four supermolecules. Adjacent

**Table 2.3**. [$N^+$–H···O] and [C–H···O] hydrogen bonding parameters *a*-*d* and centroid–centroid separations (Å) for pairs of aromatic rings in the four independent [TB24C8·**7**]$PF_6$ supermolecules (Figure 2.8) that exist in the solid state.

| | **Supermolecule** | | | |
|---|---|---|---|---|
| ***Interaction*** | **a** | **b** | **c** | **d** |
| *H Bonding* | | | | |
| *a* | | | | |
| [$N^+$···O] (Å) | 2.91 | 2.96 | 2.98 | 2.92 |
| [H···O] (Å) | 2.03 | 2.08 | 2.11 | 2.03 |
| [$N^+$–H···O] (°) | 165 | 167 | 163 | 169 |
| *b* | | | | |
| [$N^+$···O] (Å) | 3.05 | 3.04 | 2.99 | 3.00 |
| [H···O] (Å) | 2.20 | 2.16 | 2.13 | 2.13 |
| [$N^+$–H···O] (°) | 158 | 164 | 159 | 164 |
| *c* | | | | |
| [C···O] (Å) | 3.34 | 3.29 | — | 3.27 |
| [H···O] (Å) | 2.51 | 2.33 | — | 2.31 |
| [C–H···O] (°) | 144 | 175 | — | 178 |
| *d* | | | | |
| [C···O] (Å) | 3.16 | 3.14 | 3.12 | 3.19 |
| [H···O] (Å) | 2.32 | 2.33 | 2.18 | 2.43 |
| [C–H···O] (°) | 146 | 141 | 160 | 136 |
| [cat···cat] | | | | |
| [A···C] | 7.67 | 7.93 | 7.90 | 7.66 |
| [D···E] | 7.96 | 8.64 | 7.86 | 8.09 |
| [cat···Ph] | | | | |
| [A···B] | 3.86 | 3.71 | 3.86 | 3.55 |
| [B···C] | 3.96 | 4.23 | 4.22 | 4.12 |

**Table 2.4**. Hydrogen bond lengths (Å) for the interactions between the F atoms of the $PF_6^-$ anions and the H atoms located on either the $\mathbf{7}^+$ cation or the TB24C8 ring in the four independent [TB24C8·**7**]$PF_6$ supermolecules that exist in the solid state.

| | Supermolecule | | | |
|---|---|---|---|---|
| ***Interaction*** | **a** | **b** | **c** | **d** |
| [F···H(*m*-Ph)] | 2.60 | 2.45 | 2.47 | 2.55 |
| [F···H(*m*-Ph)] | 2.55 | 2.60 | 2.55 | — |
| | 2.55 | — | — | — |
| [F···H(*o*-cat)] | 2.56 | 2.34 | 2.52 | 2.43 |
| [F···H(polyether)] | 2.55 | 2.45 | 2.47 | 2.35 |
| | 2.59 | 2.54 | 2.55 | 2.57 |
| | 2.49 | — | 2.57 | 2.59 |
| | — | — | 2.55 | 2.58 |

layers—related by $C_2$ symmetry—are almost in register, thereby encapsulating[31] the $PF_6^-$ anions. Each anion participates in at least five [C–H···F] interactions, involving no fewer than four of its F atoms, to hydrogen bond donors located in (i) the benzo rings, (ii) the ethyleneoxy linkages of TB24C8, and (iii) the phenyl rings of the $\mathbf{7}^+$ cation.

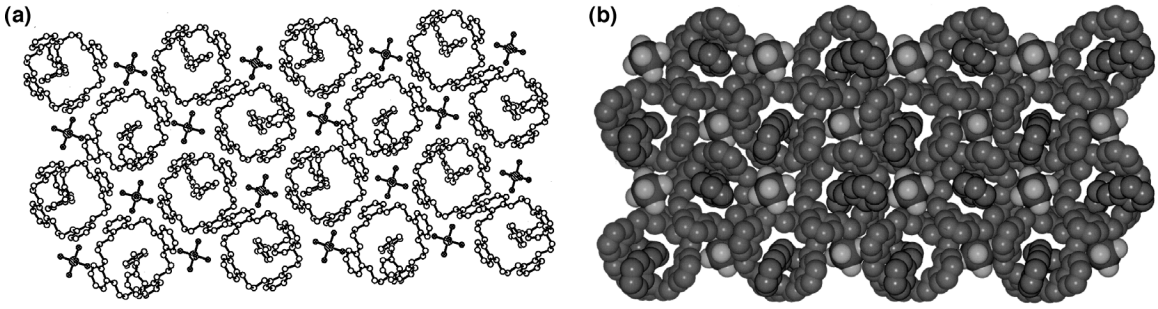


**Figure 2.9**. (**a**) Ball-and-stick and (**b**) space-filling representations (hydrogen atoms omitted for clarity) showing the layer structure of [**4**·**7**]$PF_6$.

Although initially the goal was to explore this crown ether's ability to bind $R_2NH_2^+$ ions, as the investigations proceeded it became apparent that TB24C8 was an intriguing compound in its own right. The solid-state superstructures of both solvated (MeCN)[32] and 'free' TB24C8 were determined.[33] Although both superstructures exhibit cooperative C–H···$\pi$ interactions,[34–37] in the latter, the superstructure is dominated

totally by these interactions involving both faces of all the benzo rings in such a manner that the resulting three-dimensional superstructure is held together by an array of Ar–H···$\pi$···H–CHO motifs.

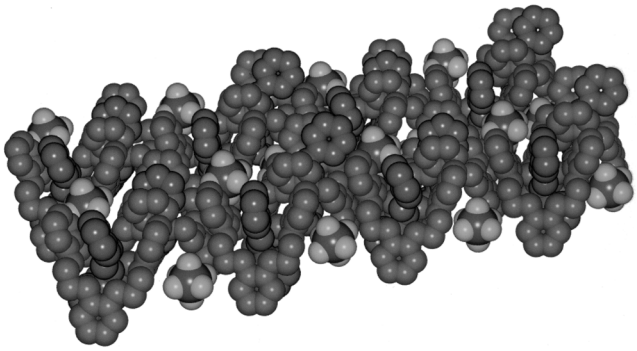

**Figure 2.10**. A space-filling representation (hydrogen atoms omitted for clarity) of [**4**·**7**]$PF_6$ showing the embedding of the $PF_6^-$ anions into the egg box-like clefts formed in the layer structure of [2]pseudorotaxane supermolecules.

Crystals of TB24C8·2MeCN were grown by vapor diffusion of $Et_2O$ into an MeCN solution of TB24C8. The X-ray analysis (Figure 2.11) of these crystals showed them to be an acetonitrile solvate in which the crown ether has a tennis ball seam-like conformation with approximate $D_{2d}$ symmetry. Rings A and B, and C and D have centroid···centroid separations of 8.05 and 7.30 Å, respectively, and associated inter-ring cleft angles of 41 (A/B) and 36° (C/D). Within these clefts are inserted the two MeCN solvent molecules, each of which are held in place by weak C–H···O hydrogen bonds between one of their methyl hydrogen atoms and a proximal catechol oxygen atom on the TB24C8 rings; the C–H···O hydrogen bond geometries are C···O, H···O (Å), C–H···O (°), 3.35, 2.45, 153 and 3.56, 2.58, 177, respectively. There are no $\pi$-$\pi$ interactions involving the cyano groups. Although the presence of the included MeCN molecules inhibits intercomplex $\pi$-$\pi$ stacking interactions, notably there are intercomplex

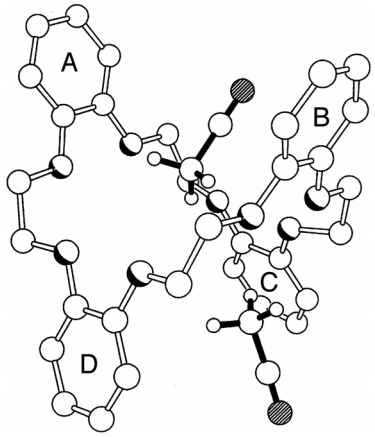


**Figure 2.11**. The solid-state superstructure of TB24C8·2MeCN.

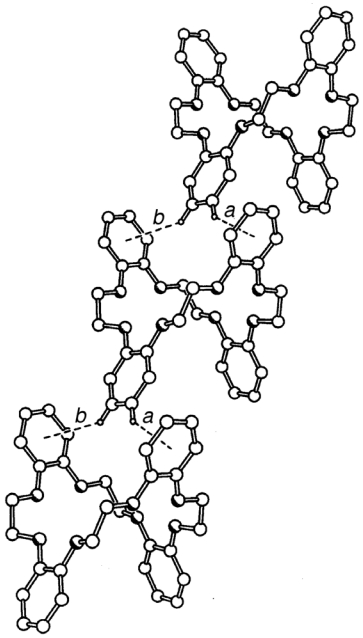


**Figure 2.12**. The C–H···$\pi$-linked supramolecular chain formed by TB24C8·2MeCN in the solid state.

C–H···$\pi$ interactions. In one instance, one of the polyether methylene hydrogen atoms in one molecule interacts with the $\pi$-system of ring A in another (H···$\pi$ 2.91 Å, C–H···$\pi$ 140°), and there is also an aromatic-aromatic edge-to-face interaction between ring B in one molecule and ring C in another (centroid···centroid separation 5.09 Å, with an associated C–H···$\pi$ geometry of H···$\pi$ 2.86 Å and C–H···$\pi$ 157°). Perhaps the most elegant intermolecular interactions are associated with the insertion of ring C of one molecule into the cleft formed between rings A and B of another (the A···C and B···C centroid···centroid separations are 5.12 and 4.99 Å, respectively) to form a supramolecular chain (Figure 2.12) which is stabilized by pairs of cooperative C–H···$\pi$ interactions (*a*: H···$\pi$ 3.16 Å, C–H···$\pi$ 136° and *b*: H···$\pi$ 2.93 Å, C–H···$\pi$ 142°).

Crystals of TB24C8 grown by vapor diffusion of $Et_2O$ into a $CHCl_3$ solution of TB24C8 produced crystals free of included solvent. Here, the crown ether adopts a conformation (Figure 2.13) that is totally different from that present in TB24C8·2MeCN, the molecule now having a distinctly 'flattened-out' and self-filling conformation with crystallographic $C_i$ symmetry in which rings A

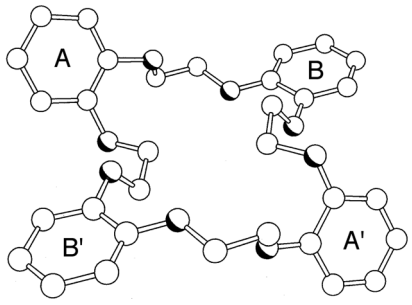


**Figure 2.13**. The solid-state structure of TB24C8.

and B are inclined by 59° to each other. This dramatic change in conformation—in comparison with that observed in the acetonitrile solvate—represents a departure from the conventional planar geometry[38] that extends from the catechol units to include the two adjacent *O*-methylene groups in each $OCH_2CH_2O$ linkage in TB24C8·2MeCN to one in which there is an approximately orthogonal relationship between the planes of the catechol rings and one or both of the associated $O–CH_2$ bonds in each of the four $OCH_2CH_2O$ linkages in the unsolvated TB24C8. The absence of solvent, coupled with the change in conformation, gives rise to a crystal packing that is totally dominated/controlled by cooperative C–H···$\pi$ interactions that involve all four catechol rings. These interactions fall into two distinct categories – (i) those utilizing aryl methine hydrogen atoms *meta* to the catechol oxygen atoms to link (Figure 2.14a) the molecules to

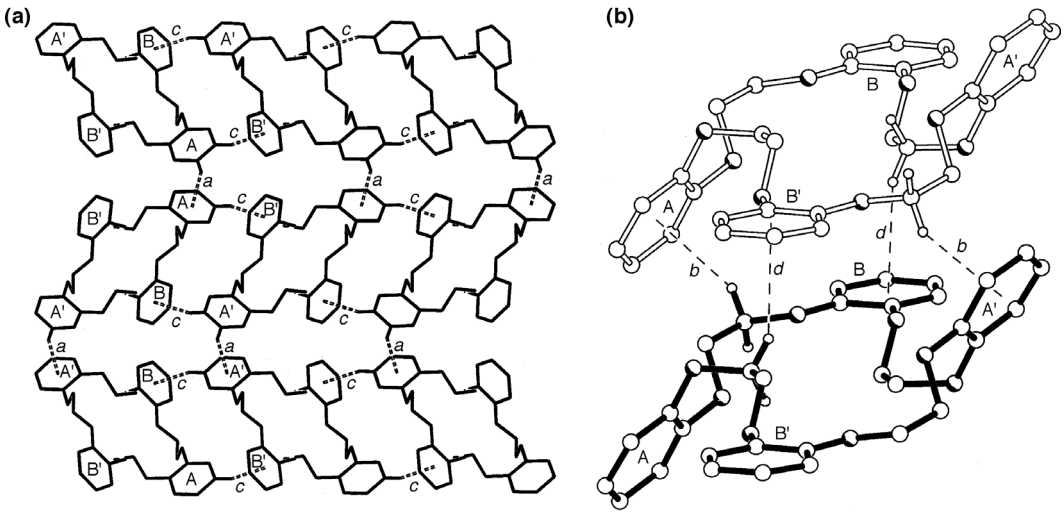


**Figure 2.14**. (**a**) Part of one of the C–H···$\pi$ (aryl methine)-linked sheets of molecules present in the solid-state superstructure of TB24C8, and (**b**) the linking of the adjacent sheets by means of C–H···$\pi$ (*O*–methylene) interactions.

form sheets, and (ii) those involving methylene hydrogen atoms to link adjacent sheets (Figure 2.14b). Another key feature of this C–H···$\pi$-linked superstructure is that all four

catechol rings have H···$\pi$ approaches to both of their faces. In each instance, there is (Figure 2.15) an aryl methine proton approaching one face of a catechol ring, and an *O*-methylene proton approaching the other (C–H···$\pi$ geometries {H···$\pi$, C–H···$\pi$}: *a* 2.83 Å, 156°; *b* 2.84 Å, 152°; *c* 2.76 Å, 154°; *d* 2.82 Å 145°). In the case of all four catechol rings, the pairs of H···$\pi$ vectors (*a*:*b* 171° and *c*:*d* 174°) are almost co-linear. It is perhaps surprising that, for a molecule possessing four aryl ring systems, there are no face-to-face $\pi$–$\pi$ interactions.[39]

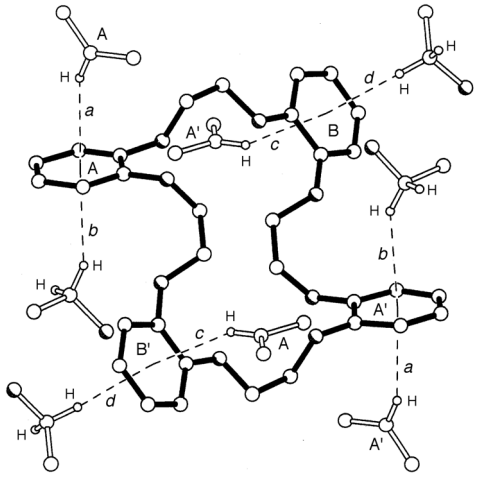


**Figure 2.15**. The systematic approaches of the aryl-methine and *O*-methylene protons to the opposite faces of all four catechol rings (A, A', B and B') in the solid-state superstructure of TB24C8.

### *2.5.3. Benzometaphenylene[25]crown-8 (BMP25C8)*

Single crystals of the [2]pseudorotaxane [**5**·**7**]$PF_6$, suitable for X-ray crystallographic analysis, were obtained from a $CD_2Cl_2$ solution of an equimolar mixture of **5** and **7**·$PF_6$ upon layering with hexanes. The 1:1 complex formed between the dibenzylammonium cation and BMP25C8 shows (Figure 2.16) the ion to be threaded through the center of the polyether macrocycle which has an extended

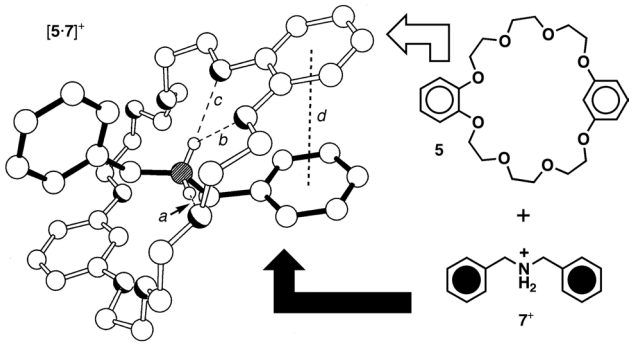


**Figure 2.16**. The X-ray crystal superstructure of the [2]pseudorotaxane [**5**·**7**-H]$^+$ formed between BMP25C8 (**5**) and the dibenzylammonium cation **7**$^+$. Hydrogen bonding distances and angles {[$N^+$···O], [H···O] distances (Å), [$N^+$–H···O] angles (°)}: (*a*) 2.91, 2.06, 156; (*b*) 2.94, 2.31, 127; (*c*) 3.08, 2.21, 162.

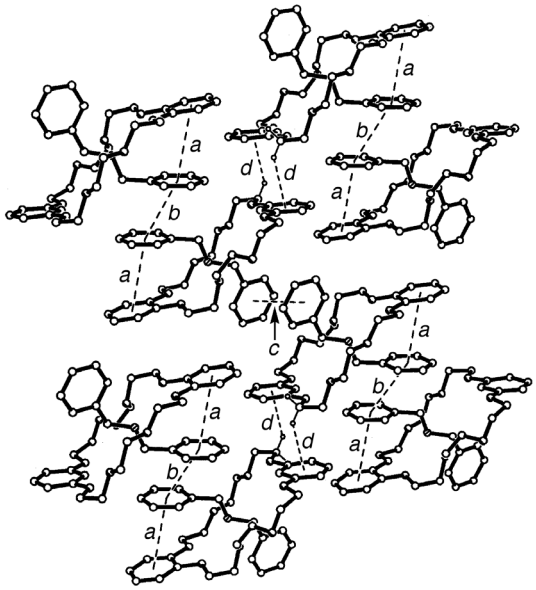


**Figure 2.17**. The sheet-like superstructure formed by the [2]pseudorotaxanes [**5**·**7**]$^+$. The geometries of the $\pi$–$\pi$ stacking interactions are (*a*) centroid-centroid distance 4.02 Å, rings inclined by 12°; (*b*) centroid-centroid distance 4.52 Å, mean interplanar separation 3.68 Å; (*c*) centroid-centroid distance 3.99 Å, mean interplanar separation 3.71 Å. The C–H···$\pi$ interaction (*d*) is characterized by an H–$\pi$ distance of 2.84 Å and a C–H···$\pi$ angle of 140°.

geometry similar to that in its uncomplexed state. The two phenyl rings in the cation are both fairly steeply inclined (by 41 and 68°, respectively) to the near-planar, all-*anti* $CCH_2NH_2^+CH_2C$ backbone. Stabilization of the [2]pseudorotaxane is *via* $N^+$–H···O hydrogen bonding, supplemented by a weak $\pi$–$\pi$ stacking interaction (*d* in Figure 2.16) between the catechol ring in the crown ether macrocycle and one of the phenyl rings of the cation. These two ring systems are inclined by *ca*. 12° and have a centroid-centroid separation of 4.02 Å. The [2]pseudorotaxanes are linked *via* a combination of $\pi$–$\pi$ and C–H···$\pi$ interactions to form sheets as illustrated in Figure 2.17. There are no obvious interactions involving the $PF_6^-$ ions.

Once again, although initially the goal was to explore this crown ether's ability to bind $R_2NH_2^+$ ions, it became apparent that the 'free' macrocycle was interesting in its own right. Single crystals suitable for X-ray crystallographic analysis were grown from an ethanolic solution upon slow evaporation. The X-ray analysis of BMP25C8 (**5**) shows (Figure 2.18a) the macrocycle to have an extended geometry with a fairly large central pathway through the center of the macroring. The molecules stack along the

crystallographic *b* direction and are linked *via* pairs of C–H···$\pi$ interactions (*a* and *b* in Figure 2.18b) involving one of the phenoxymethylene hydrogen atoms of both the catechol and resorcinol rings and their adjacent counterparts within the stack. These

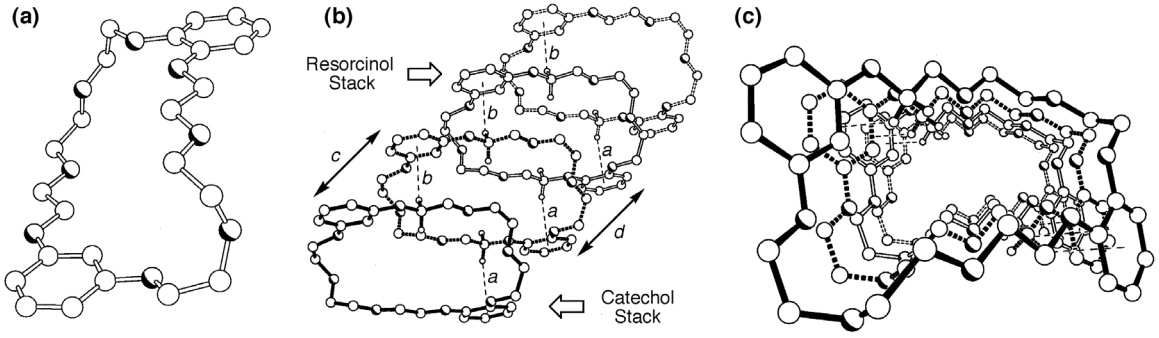


**Figure 2.18**. (**a**) The crystal structure of BMP25C8 **5**. (**b**) Adjacent molecules are stacked by virtue of pairs of C–H···$\pi$ interactions, (*a*) H···$\pi$ distance 2.85 Å, C–H···$\pi$ angle 140°; (*b*) H···$\pi$ distance 2.79 Å, C–H···$\pi$ angle 137°, supplemented by $\pi$–$\pi$ stacking interactions between the resorcinol and catechol moieties, interactions *c* and *d*, respectively. (**c**) End-on view of the constricted nanotube formed by the stacking of BMP25C8 macrocycles.

interactions are supplemented, to a lesser degree, by partial $\pi$–$\pi$ overlap between the resorcinol rings and between the catechol rings (*c* and *d* in Figure 2.18b) of adjacent molecules (the centroid-centroid and interplanar separations are 5.14, 3.44 Å and 5.14, 3.52 Å, respectively). The combination of these intermolecular interactions produces (Figure 2.18c) constricted nanotubes that extend through the crystal. Adjacent nanotubes, in one direction in the crystal, are crosslinked *via* an additional C–H···$\pi$ interaction between one of the resorcinol phenoxymethylene hydrogen atoms in one stack and a catechol ring in the next (the H···$\pi$ distance is 2.91 Å and the C–H···$\pi$ angle 148°).

## 2.6. Conclusions

Thus, it has been shown that certain crown ethers[40] with either [24]crown-8 or [25]crown-8 constitutions bind *para*-disubstituted dibenzylammonium ions in solution,

the ‘gas phase’, and the solid state, as evidenced by $^1$H NMR spectroscopy, LSIMS, and X-ray crystallography, respectively. When considering the [24]crown-8 analogues, as more aromatic residues are appended to the macrocyclic framework, the affinity of the crown ethers toward the dibenzylammonium ions is diminished and, in the case of TB24C8 (**4**), no appreciable binding in solution could be detected. Moreover, increasing the size of the macrocyclic polyether ring from 24 to 25 atoms—necessarily disrupting the O–C–C–O repeating unit—reduces the $K_a$ values for the formation of [2]pseudorotaxanes, demonstrating that not only substitution effects, but also relatively small changes in constitution, can alter dramatically the crown ether’s ability to encircle the secondary dibenzylammonium ion center.

Despite its negligible affinity for secondary ammonium ions in solution, TB24C8 has proven to be an interesting compound in other respects. It is noteworthy that, in the solid-state superstructures of both TB24C8 and TB24C8·2MeCN, although both the *O*–methylene and Ar–H protons have the option (which they avoid) of forming hydrogen bonds to oxygen atoms—which represent better hydrogen bond acceptors than π-systems[41]—and the benzo rings have the opportunity to interact in a face-to-face π–π stacking manner, the three-dimensional superstructure is dominated solely by C–H···π interactions. The exclusive use of this motif could result for a number of reasons, including (i) the phenolic nature of *all* of the oxygen atoms in the TB24C8 macroring which reduces their propensity to act as effective hydrogen bond acceptors, (ii) edge-to-face geometries which are favored over their face-to-face alternatives because the small surface area of the catechol rings enhances the electrostatic interactions in preference to

dispersive ones,[39,42] and finally (iii) the C–H···$\pi$ networks, which extend throughout each solid-state superstructure and are thus associated with extensive positive cooperativity.[43,44] Although perhaps the weakest of hydrogen bonds, the role played by C–H···$\pi$ interactions in molecular recognition events is undoubtedly an important one, and is highlighted in the solid-state superstructures of both TB24C8 and TB24C8·2MeCN. If there is a take-home message from these investigations of the idiosyncrasies of TB24C8 in the solid state, it is that the weak C–H···$\pi$ hydrogen bond should not be overlooked when considering noncovalent bonding interactions, as it may be present more often than we think. As Nishio has commented,[45] a considerable portion of what in the past may have been imprecisely defined as 'hydrophobic interactions' could well be as a consequence of C–H···$\pi$ interactions.

However, as demonstrated in the case of [TB24C8·**7**]$PF_6$, this weak noncovalent interaction can be usurped easily by other—more enthalpically favorable—interactions. This solid-state superstructure appears to be determined by a plethora of stabilizing C–H···F hydrogen bonding interactions to highly ordered, interstitially located, $PF_6^-$ anions at the expense of an extended C–H···$\pi$ network.

## 2.7. Experimental

**General:** Chemicals—including DB24C8 (**3**)—were purchased from Aldrich and used as received unless indicated otherwise. The crown ethers 24C8 (**1**)[13], B24C8 (**2**),[14] and TB24C8 (**4**),[16] and dibenzylammonium salts **7**·$PF_6$[8b] and **8**·$PF_6$[12] were prepared according to literature procedures. Solvents were dried according to literature procedures.[46] Thin-layer chromatography was carried out using aluminium sheets precoated with silica gel 60F (Merck

5554). The plates were inspected by UV light and, if required, developed in $I_2$ vapor. Column chromatography was carried out using silica gel 60F (Merck 9385, 0.040–0.063 mm). Melting points were determined on an Electrothermal 9100 apparatus and are uncorrected. $^1$H and $^{13}$C NMR spectra were recorded on either a Bruker AC300 (300 and 75 MHz, respectively), Bruker ARX400 (400 and 100 MHz, respectively), or Bruker ARX500 (500 and 125 MHz, respectively) spectrometer, using residual solvent as the internal standard. All chemical shifts are quoted on the $\delta$ scale, and all coupling constants are expressed in Hertz (Hz). Liquid secondary ion (LSI) mass spectra were obtained on a VG Zabspec mass spectrometer, equipped with a cesium ion source and utilizing a *m*-nitrobenzyl alcohol matrix. Fast atom bombardment (FAB) mass spectra were obtained using a ZAB-SE mass spectrometer, equipped with a krypton primary atom beam, utilizing a *m*-nitrobenzyl alcohol matrix. Cesium iodide or poly(ethylene glycol) were employed as reference compounds. Microanalyses were performed by either the University of North London Microanalytical Service (UK) or Quantitative Technologies, Inc (USA).

**1,3-Bis(2-{2-[2-(2-*p*-tolylsulfonyloxy)ethoxy]ethoxy}ethoxy)benzene (11)**. 1,3-Bis(2-{2-[2-(2-hydroxy)ethoxy]ethoxy}ethoxy)benzene **10**[17] (10.0 g, 26.7 mmol), $Et_3N$ (27.0 g, 267 mmol), and a catalytic quantity of DMAP were dissolved in anhydrous $CH_2Cl_2$ (100 mL). This solution was cooled down to 0 °C in an ice bath and TsCl (25.5 g, 134 mmol) dissolved in dry $CH_2Cl_2$ (100 mL) was added dropwise over a 3 h period. The reaction mixture was allowed to warm up to ambient temperature before being stirred overnight. Hydrochloric acid (5N, 200 mL) was added carefully to the reaction mixture before the organic phase was recovered and washed with 2N HCl (200 mL) and saturated brine (200 mL). This solution was then dried ($MgSO_4$) and the solvents were removed *in vacuo* to afford a dark yellow oil, which was purified by chromatography ($SiO_2$: gradient elution with $CH_2Cl_2$ to 1:1 $CH_2Cl_2$/EtOAc) to yield the title compound as a pale yellow oil (11.8 g, 64 %); $^1$H NMR (300 MHz, $CDCl_3$): $\delta$ = 2.42 (s, 6H), 3.56–3.87 (m, 16H), 4.04–4.19 (m, 8H), 6.45–6.54 (m, 3H), 7.14 (t, $J$ = 8.3 Hz, 1H), 7.32 (d, $J$ = 8.2 Hz, 4H), 7.79 (d, $J$ = 8.2 Hz, 4H); $^{13}$C NMR (75 MHz, $CDCl_3$): $\delta$ = 21.7, 67.5, 68.8, 69.4, 69.9, 70.9, 101.9, 107.2, 128.1, 130.0, 133.1, 145.0, 160.1; MS (FAB): *m/z* = 683 $[M+H]^+$; $C_{32}H_{42}O_{12}S_2$ (682.8): calcd C 56.29, H 6.20; found C 56.12, H 6.24.

**Benzometaphenylene[25]crown-8** (**5**). A solution of the ditosylate **11** (5.0 g, 7.3 mmol) and catechol (0.81 g, 7.3 mmol) in dry MeCN (500 mL) was added dropwise over a 3 d period to a suspension of $Cs_2CO_3$ (11.9 g, 36.6 mmol) in refluxing MeCN (500 mL). After 4 d of heating under reflux, the reaction mixture was allowed to cool down. Subsequently, it was filtered to remove inorganic salts. The filtrate was evaporated to dryness and the residue partitioned between $CH_2Cl_2$ (250 mL) and an aqueous $K_2CO_3$ solution (10 % w/v, 250 mL). The organic phase was then washed with a further aliquot of aqueous $K_2CO_3$, before being dried ($MgSO_4$). The solvents were removed *in vacuo* and the crude product was subjected to chromatography ($SiO_2$: EtOAc/hexane 9:1), yielding BMP25C8 (**5**) as a white solid (2.73 g, 83 %); M.p. 66–68 °C; $^1$H NMR (400 MHz, $CDCl_3$): $\delta$ = 3.71–3.75 (m, 8H), 3.81–3.87 (m, 8H), 4.13–4.16 (m, 8H), 6.50 (dd, $J$ = 2.4, 8.0 Hz, 2H), 6.70 (t, $J$ = 2.4 Hz, 1H); 6.89–6.92 (m, 4H), 7.12 (t, $J$ = 8.0 Hz, 1H); $^{13}$C NMR (100 MHz, $CDCl_3$): $\delta$ = 68.1, 69.1, 70.0, 71.0, 71.1, 102.8, 107.9, 115.3, 121.8, 129.8, 149.1, 160.1; MS (FAB): *m/z* = 449 $[M+H]^+$; $C_{24}H_{32}O_8$ (448.5): calcd C 64.27, H 7.19; found C 64.33, H 7.12.

*Crystal data for* **5**: $C_{24}H_{32}O_8$, $M$ = 448.5, monoclinic, space group $P2_1/c$ (no. 14), $a$ = 17.974(2), $b$ = 5.140(1), $c$ = 24.851(3) Å, $\beta$ = 92.93(1)°, $V$ = 2292.8(4) Å$^3$, $Z$ = 4, $\rho_c$ = 1.299 g cm$^{-3}$, $\mu(Mo_{K\alpha})$ = 0.97 cm$^{-1}$, $F(000)$ = 960, $T$ = 293 K; clear prismatic needles, 0.83 x 0.40 x 0.27 mm, Siemens P4/PC diffractometer, graphite-monochromated $Mo_{K\alpha}$ radiation, $\omega$-scans, 4028 independent reflections. The structure was solved by direct methods and the non-hydrogen atoms were refined anisotropically. The C–H hydrogen atoms were placed in calculated positions, assigned isotropic thermal parameters, $U(H) = 1.2U_{eq}(C)$, and allowed to ride on their parent atoms. Refinements were by full matrix least-squares based on $F^2$ to give $R_1$ = 0.062, $wR_2$ = 0.151 for 2493 independent observed reflections [$|F_o| > 4\sigma(|F_o|)$, $2\theta \leq 50°$] and 289 parameters. All computations were carried out using the SHELXTL PC program system.[47] CCDC 138346.[48]

**Bis(4-methoxycarbonylbenzyl)ammonium Hexafluorophosphate** (**9**·$PF_6$). A solution of bis(4-methoxycarbonylbenzyl)amine **9**[9b] (1.0 g, 3.2 mmol) in MeOH (50 mL) was treated with 5N HCl (10 mL) and the solvents were removed *in vacuo*. The resulting white solid was

dissolved in $H_2O$ (50 mL) and an excess of $NH_4PF_6$ was added until no further precipitation occurred. Filtration afforded the title compound as a white solid (1.35 g, 92 %); M.p. 240–242 °C; $^1$H NMR (400 MHz, $CD_3CN$): $\delta$ = 3.88 (s, 6H), 4.31 (s, 4H), 7.55–7.59 (m, 4H); 8.04-8.08 (m, 4H); $^{13}$C NMR (100 MHz, $CD_3CN$): $\delta$ = 52.2, 53.1, 130.9, 131.5, 132.6, 136.1, 167.2; MS (FAB): *m/z* = 314 $[M–PF_6]^+$; $C_{18}H_{20}F_6NO_4P$ (459.3): calcd C 47.07, H 4.39, N 3.05; found C 47.12, H 4.28, N 2.84.

*Crystal data for* [TB24C8·**7**]$PF_6$: Crystals of [TB24C8·**7**]$PF_6$ were grown by slow evaporation of a $CHCl_3$/MeCN/*n*-$C_6H_{14}$ solution (7:3:3) containing an equimolar mixture of TB24C8 and **7**·$PF_6$. $[C_{46}H_{48}NO_8]PF_6$·0.5MeCN·0.125$CH_2Cl_2$, $M$ = 919.0, triclinic, space group $P\bar{1}$ (no. 2), $a$ = 14.182(1), $b$ = 23.357(2), $c$ = 28.107(2) Å, $\alpha$ = 91.51(1), $\beta$ = 90.51(1), $\gamma$ = 104.37(1)°, $V$ = 9015(1) Å$^3$, $Z$ = 8 (there are four crystallographically independent 1:1 complexes in the asymmetric unit), $\rho_c$ = 1.354 g cm$^{-3}$, $\mu$($Cu_{K\alpha}$) = 13.7 cm$^{-1}$, $F$(000) = 3842, $T$ = 183 K; clear platy prisms, 0.43 x 0.20 x 0.07 mm, Siemens P4 rotating anode diffractometer, graphite-monochromated $Cu_{K\alpha}$ radiation, $\omega$-scans, 24143 independent reflections. The structure was solved by direct methods and all the full occupancy non-hydrogen atoms were refined anisotropically. Disorder was found in the thread component of one of the four crystallographically independent [2]pseudorotaxanes and in one of the included acetonitrile solvent molecules; in each case two partial occupancy orientations were identified with only the non-hydrogen atoms of the major occupancy orientations being refined anisotropically (the rest being refined isotropically). Refinements were by blocked full matrix least-squares based on $F^2$ to give $R_1$ = 0.089, $wR_2$ = 0.216 for 12765 independent observed reflections [$|F_o| > 4\sigma(|F_o|)$, $2\theta \leq 115°$] and 2264 parameters. CCDC 132801.[48]

*Crystal data for* TB24C8·2MeCN: Crystals of TB24C8·2MeCN were grown by vapor diffusion of $Et_2O$ into MeCN solution of TB24C8. $C_{32}H_{32}O_8$·2MeCN, $M$ = 626.7, monoclinic, $P2_1/c$ (no. 14), $a$ = 16.018(1), $b$ = 10.200(2), $c$ = 21.394(2) Å, $\beta$ = 108.24(1)°, $V$ = 3319.7(7) Å$^3$, $Z$ = 4, $\rho_c$ = 1.254 g cm$^{-3}$, $\mu$($Cu_{K\alpha}$) = 7.28 cm$^{-1}$, $F$(000) = 1328, $T$ = 173 K; clear plates, 0.93 x 0.47 x 0.10 mm, Siemens P4 rotating anode diffractometer, $\omega$-scans, 5198 independent reflections. The structure was solved by direct methods and the non-

hydrogen atoms were refined anisotropically using full matrix least-squares based on $F^2$ to give $R_1 = 0.063$, $wR_2 = 0.150$ for 3570 independent observed reflections [$|F_o| > 4\sigma(|F_o|)$, $2\theta \leq 124°$] and 416 parameters. CCDC 132743.[48]

*Crystal data for* TB24C8: Crystals of TB24C8 were grown by vapor diffusion of $Et_2O$ into $CHCl_3$ solution of TB24C8. $C_{32}H_{32}O_8$, $M = 544.6$, monoclinic, $P2_1/c$ (no. 14), $a = 9.585(2)$, $b = 18.931(2)$, $c = 7.297(1)$ Å, $\beta = 94.29(1)°$, $V = 1320.3(3)$ Å$^3$, $Z = 2$ (the molecule has crystallographic $C_i$ symmetry), $\rho_c = 1.370$ g cm$^{-3}$, $\mu(Cu_{K\alpha}) = 8.07$ cm$^{-1}$, $F(000) = 576$, $T = 293$ K; clear plates, 0.50 x 0.47 x 0.13 mm, Siemens P4/PC diffractometer, $\omega$-scans, 2077 independent reflections. The structure was solved by direct methods and the non-hydrogen atoms were refined anisotropically using full matrix least-squares based on $F^2$ to give $R_1 = 0.049$, $wR_2 = 0.134$ for 1713 independent observed reflections [$|F_o| > 4\sigma(|F_o|)$, $2\theta \leq 124°$] and 182 parameters. CCDC 132744.[48]

*Crystal data for* [**5**·**7**]$PF_6$: $[C_{38}H_{48}NO_8][PF_6]$, $M = 791.7$, triclinic, space group $P\bar{1}$ (no. 2), $a = 11.265(1)$, $b = 12.853(3)$, $c = 14.495(2)$ Å, $\alpha = 104.12(2)$, $\beta = 102.72(1)$, $\gamma = 96.53(2)°$, $V = 1954.1(6)$ Å$^3$, $Z = 2$, $\rho_c = 1.346$ g cm$^{-3}$, $\mu(Mo_{K\alpha}) = 1.50$ cm$^{-1}$, $F(000) = 832$, $T = 293$ K; clear prisms, 0.57 x 0.33 x 0.13 mm, Siemens P4/PC diffractometer, graphite-monochromated $Mo_{K\alpha}$ radiation, $\omega$-scans, 5696 independent reflections. The structure was solved by direct methods. Disorder was found in one of the polyether arms and this was resolved into two partial occupancy orientations with the non-hydrogen atoms of the major occupancy orientation being refined anisotropically (those of the minor occupancy orientation were refined isotropically). The remaining non-hydrogen atoms were refined anisotropically. The N–H hydrogen atoms were located from a $\Delta F$ map and allowed to refine isotropically subject to an N–H distance constraint. The C–H hydrogen atoms were placed in calculated positions, assigned isotropic thermal parameters, $U(H) = 1.2U_{eq}(C)$, and allowed to ride on their parent atoms. Refinements were by full matrix least-squares based on $F^2$ to give $R_1 = 0.083$, $wR_2 = 0.201$ for 2613 independent observed reflections [$|F_o| > 4\sigma(|F_o|)$, $2\theta \leq 47°$] and 480 parameters. All computations were carried out using the SHELXTL PC program system.[47] CCDC 138347.[48]

## 2.8. References and Notes


1. Pedersen, C. J. *Angew. Chem., Int. Ed. Engl.* **1988**, *27*, 1021–1027.
2. (a) Lehn, J.-M. *Supramolecular Chemistry*; VCH: Weinheim, 1995. (b) *Comprehensive Supramolecular Chemistry*; Atwood, J. L.; Davies, J. E. D.; MacNicol, D. D.; Vögtle, F., Eds.; Pergamon: Oxford, 1996; 11 vols.
3. Pedersen, C. J. *J. Am. Chem. Soc*. **1967**, *89*, 7017–7036.
4. For in-depth and historical analyses of cation/crown ether complexation, see: (a) Bradshaw, J. S.; Izatt, R. M.; Bordunov, A. V.; Zhu, C. Y.; Hathaway, J. K. in *Comprehensive Supramolecular Chemistry, Vol. 1*; Atwood, J. L.; Davies, J. E. D.; MacNicol, D. D.; Vögtle, F.; Gokel, G. W., Eds.; Pergamon: Oxford, 1996; pp. 35–95. (b) Izatt, R. M.; Pawluk, K.; Bradshaw, J. S.; Bruening, R. L. *Chem. Rev.* **1995**, *95*, 2529–2586. (c) Izatt, R. M.; Pawluk, K.; Bradshaw, J. S.; Bruening, R. L. *Chem. Rev.* **1991**, *91*, 1721–2085. (d) Gokel, G. W. *Crown Ethers and Cryptands*; The Royal Society of Chemistry: Cambridge, 1991; pp. 64–98. (e) *Cation Binding by Macrocycles*; Inoue, Y.; Gokel G. W., Eds.; Marcel Dekker: New York, 1990. (f) Vögtle, F.; Weber, E. in *Crown Ethers and Analogs*; Patai, S.; Rappoport, Z., Eds.; Wiley, 1989; pp. 207–304. (g) Goldberg, I. in *Inclusion Compounds, Vol. 2*; Atwood, J. L.; Davies, J. E. D.; MacNicol, D. D., Eds.; Academic Press: London, 1984; pp. 261–335.
5. For some recent examples, see: (a) Drljaca, A.; Hardie, M. J.; Raston, C. L.; Spiccia, L. *Chem. Eur. J.* **1999**, *5*, 2295–2299. (b) Marchand, A. P.; Chong, H.-S.; Alihodzic, S.; Watson, W. H.; Bodige, S. G. *Tetrahedron* **1999**, *55*, 9687–9696. (c) Liu, H.; Liu, S.; Echegoyen, L. *Chem. Commun.* **1999**, 1493–1494. (d) Flink, S.; van Veggel, F. C. J. M.; Reinhoudt, D. N. *J. Phys. Chem. B* **1999**, *103*, 6515–6520. (e) Bartsch, R. A.; Hwang, H.-S.; Talanov, V. S.; Talanova, G. G.; Purkiss, D. W.; Rogers, R. D. *J. Org. Chem.* **1999**, *64*, 5341–5349.
6. In Pedersen's seminal paper (ref. 3), he noted that primary alkylammonium ions form 1:1 complexes with dibenzo[18]crown-6 (DB18C6). This ground-breaking discovery subsequently spawned much research in the areas of host-guest and supramolecular chemistry. For examples spanning from Pedersen's day until the present, see: (a) Kyba, E. B.; Koga, K.; Sousa, L. R.; Siegel, M. G.; Cram, D. J. *J. Am. Chem. Soc.* **1973**, *95*, 2692–2693. (b) Cram, D. J.; Cram, J. M. *Science* **1974**, *183*, 803–809. (c) Tarnowski, T. L.; Cram, D. J. *J. Chem. Soc., Chem. Commun.* **1976**, 661–663. (d) Timko, J. M.; Moore, S. S.; Walba, D. M.; Hiberty, P. C.; Cram, D. J. *J. Am. Chem. Soc.* **1977**, *99*, 4207–4219. (e) Kyba, E. P.; Timko, J. M.; Kaplan, L. J.; de Jong, F.; Gokel, G. W.; Cram, D. J. *J. Am. Chem. Soc.* **1978**, *100*, 4558–4568. (f) Cram, D. J.; Cram, J. M. *Acc. Chem. Res.* **1978**, *11*, 8–14. (g) Stoddart, J. F. *Chem. Soc. Rev.* **1979**, *8*, 85–142. (h) Bovill, M. J.; Chadwick, D. J.; Johnson, M. R.; Jones, N. F.; Sutherland, I. O.; Newton, R. F. *J. Chem. Soc., Chem. Commun.* **1979**, 1065–1066. (i) Lehn, J.-M. in *IUPAC Frontiers of Chemistry*; Laidler, K. J., Ed.; Pergamon: Oxford, 1982; pp. 265–272. (j) Goldberg, I. *J. Am. Chem. Soc.* **1980**, *102*,

4106-4113. (k) de Jong, F.; Reinhoudt, D. N. *Adv. Phys. Org. Chem.* **1980**, *17*, 279–433. (l) Cram, D. J.; Trueblood, K. N. *Top. Curr. Chem.* **1981**, *98*, 43–106. (m) Bradshaw, J. S.; Baxter, S. L.; Lamb, J. D.; Izatt, R. M.; Christensen, J. J. *J. Am. Chem. Soc.* **1981**, *103*, 1821–1827. (n) Trueblood, K. N.; Knobler, C. B.; Lawrence, D. S.; Stevens, R. V. *J. Am. Chem. Soc.* **1982**, *104*, 1355–1362. (o) Aldag, R.; Schröder, G. *Liebigs Ann. Chem.* **1984**, 1036–1045. (p) Sutherland, I. O. *Chem. Soc. Rev.* **1986**, *15*, 63–91. (q) Stoddart, J. F. *Top. Stereochem.* **1987**, *17*, 205–288. (r) Cram, D. J. *Angew. Chem., Int. Ed. Engl.* **1988**, *27*, 1009–1020. (s) Misumi, S. *Pure Appl. Chem.* **1990**, *62*, 493–498. (t) I. O. Sutherland, *Pure Appl. Chem.* 499–504. (u) Izatt, R. M.; Wang, T.; Hathaway, J. K.; Zhang, X. X.; Curtis, J. C.; Bradshaw, J. S.; Zhu, C. Y.; Huszthy, P. *J. Incl. Phenom.* **1994**, *17*, 157–175. (v) Reetz, M. T.; Huff, J.; Rudolph, J.; Töllner, K.; Deege, A.; Goddard, R. *J. Am. Chem. Soc.* **1994**, *116*, 11588–11589. (w) Williamson, B. L.; Creaser, C. S. *Int. J. Mass Spectrom.* **1998**, *188*, 53–61. (x) Hansson, A. P.; Norrby, P.-O.; Wärnmark, K. *Tetrahedron Lett.* **1998**, *39*, 4565–4568. (y) Tsukube, H.; Wada, M.; Shinoda, S.; Tamiaki, H. *Chem. Commun.* **1999**, 1007–1008.

7. Complexes formed between secondary dialkylammonium ions and crown ethers having less than 24 atoms in their macrorings have been observed to occur in a *face-to-face* manner. See: (a) Metcalfe, J. C.; Stoddart, J. F.; Jones, G. *J. Am. Chem. Soc.* **1977**, *99*, 8317–8319. (b) Krane, J.; Aune, O. *Acta Chem. Scand.* **1980**, *34B*, 397–401. (c) Metcalfe, J. C.; Stoddart, J. F.; Jones, G.; Atkinson, A.; Kerr, I. S.; Williams, D. J. *J. Chem. Soc., Chem. Commun.* **1980**, 540–543. (d) Abed-Ali, S. S.; Brisdon, B. J.; England, R. *J. Chem. Soc., Chem. Commun.* **1987**, 1565–1566.

8. (a) Ashton, P. R.; Campbell, P. J.; Chrystal, E. J. T.; Glink, P. T.; Menzer, S.; Philp, D.; Spencer, N.; Stoddart, J. F.; Tasker, P. A.; Williams, D. J. *Angew. Chem., Int. Ed. Engl*. **1995**, *34*, 1865–1869. (b) Ashton, P. R.; Chrystal, E. J. T.; Glink, P. T.; Menzer, S.; Schiavo, C.; Spencer, N.; Stoddart, J. F.; Tasker, P. A.; White, A. J. P.; Williams, D. J. *Chem. Eur. J*. **1996**, *2*, 709–728.

9. (a) Kolchinski, A. G.; Busch, D. H.; Alcock, N. W. *J. Chem. Soc., Chem. Commun*. **1995**, 1289–1291. (b) Ashton, P. R.; Glink, P. T.; Stoddart, J. F.; Tasker, P. A.; White, A. J. P.; Williams, D. J. *Chem. Eur. J.* **1996**, *2*, 729–736. (c) Martínez-Díaz, M.-V.; Spencer, N.; Stoddart, J. F. *Angew. Chem., Int. Ed. Engl.* **1997**, *36*, 1904–1907. (d) Ashton, P. R.; Baxter, I.; Fyfe, M. C. T.; Raymo, F. M.; Spencer, N.; Stoddart, J. F.; White, A. J. P.; Williams, D. J. *J. Am. Chem. Soc.* **1998**, *120*, 2297–2307. (e) Ashton, P. R.; Ballardini, R.; Balzani, V.; Baxter, I.; Credi, A.; Fyfe, M. C. T.; Gandolfi, M. T.; Gómez-López, M.; Martínez-Díaz, M.-V.; Piersanti, A.; Spencer, N.; Stoddart, J. F.; Venturi, M.; White, A. J. P.; Williams, D. J. *J. Am. Chem. Soc.* **1998**, *120*, 11932–11942. (f) Kolchinski, A. G.; Alcock, N. W.; Roesner, R. A.; Busch, D. H. *Chem. Commun*. **1998**, 1437–1438. (g) Cantrill, S. J.; Fulton, D. A.; Fyfe, M. C. T.; Stoddart, J. F.; White, A. J. P.; Williams, D. J. *Tetrahedron Lett*. **1999**, *40*, 3669–3672. (h) Rowan, S. J.; Cantrill, S. J.; Stoddart, J. F. *Org. Lett*. **1999**, *1*, 129–132. (i) Takata, T.; Kawasaki, H.; Asai, S.; Furusho, Y.; Kihara, N. *Chem. Lett*. **1999**, 223–224. (j) Cantrill, S. J.; Rowan, S. J.; Stoddart, J.

F. *Org. Lett*. **1999**, *1*, 1363–1366. (k) Cao, J.; Fyfe, M. C. T.; Stoddart, J. F.; Cousins, G. R. L.; Glink, P. T. *J. Org. Chem*. **2000**, *65*, 1937-1946. (l) Rowan, S. J.; Stoddart, J. F. *J. Am. Chem. Soc*. **2000**, 122, 164-165. (m) Furusho, Y.; Hasegawa, T.; Tsuboi, A.; Kihara, N.; Takata, T. *Chem. Lett*. **2000**, 18-19. (n) Kihara, N.; Yuya, T.; Kawasaki, H.; Takata, T. *Chem. Lett*. **2000**, 506-507.

10. (a) Ashton, P. R.; Glink, P. T.; Martínez-Díaz, M.-V.; Stoddart, J. F.; White, A. J. P.; Williams, D. J. *Angew. Chem., Int. Ed. Engl.* **1996**, *35*, 1930–1933. (b) Ashton, P. R.; Collins, A. N.; Fyfe, M. C. T.; Menzer, S.; Stoddart, J. F.; Williams, D. J. *Angew. Chem., Int. Ed. Engl.* **1997**, *36*, 735–739. (c) Ashton, P. R.; Fyfe, M. C. T.; Hickingbottom, S. K.; Menzer, S.; Stoddart, J. F.; White, A. J. P.; Williams, D. J. *Chem. Eur. J.* **1998**, *4*, 577–589. (d) Fyfe, M. C. T.; Stoddart, J. F. *Coord. Chem. Rev*. **1999**, *183*, 139–155. (e) Yamaguchi, N.; Gibson, H. W. *Angew. Chem., Int. Ed*. **1999**, *38*, 143–147. (f) Yamaguchi, N.; Gibson, H. W. *Chem. Commun*. **1999**, 789–790.
11. (a) Philp, D.; Stoddart, J. F. *Synlett* **1991**, 445–458. (b) Whitesides, G. M.; Mathias, J. P.; Seto, C. T. *Science*, **1991**, *154*, 1312–1319. (c) Lawrence, D. S.; Jiang, T.; Levett, M. *Chem. Rev.* **1995**, *95*, 2229–2260. (d) Philp, D.; Stoddart, J. F. *Angew. Chem., Int. Ed. Engl.* **1996**, *35*, 1154–1196. (e) Stang, P. J.; Olenyuk, B. *Acc. Chem. Res.* **1997**, *30*, 502–518. (f) Cusack, L.; Rao, S. N.; Wenger, J.; Fitzmaurice, D. *Chem. Mater.* **1997**, *9*, 624–631. (g) Conn, M. M.; Rebek, Jr., J. *Chem. Rev.* **1997**, *97*, 1647–1668. (h) Linton, B.; Hamilton, A. D. *Chem. Rev.* **1997**, *97*, 1669–1680. (i) Fujita, M. *Chem. Soc. Rev.* **1998**, *27*, 417–425. (j) Breen, T. L.; Tien, J.; Oliver, S. R. J.; Hadzic, T.; Whitesides, G. M. *Science* **1999**, *284*, 948–951. (k) Tomalia, D. A.; Wang, Z. G.; Tirrel, M. *Curr. Opin. Colloid Interface Sci.* **1999**, *4*, 3–5. (l) Emrick, T.; Fréchet, J. M. J. *Curr. Opin. Colloid Interface Sci.* **1999**, *4*, 15–23. (m) Sijbesma, R. P.; Meijer, E. W. *Curr. Opin. Colloid Interface Sci.* **1999**, *4*, 24–32.
12. Ashton, P. R.; Fyfe, M. C. T.; Hickingbottom, S. K.; Stoddart, J. F.; White, A. J. P.; Williams, D. J. *J. Chem. Soc., Perkin Trans. 2* **1998**, 2117–2128.
13. Inoue, Y.; Liu, Y.; Amano, F.; Ouchi, M.; Tai, A.; Hakushi, T. *J. Chem. Soc., Dalton Trans.* **1988**, 2735–2738.
14. Although the synthesis of B24C8 (**2**) has been reported previously, (Czech, B. P.; Czech, A.; Knudsen, B. E.; Bartsch, R. A. *Gazz. Chim. Ital*. **1987**, *12*, 717–722) a modified procedure was adopted to prepare **2**. The required ditosylate was prepared in two steps (i, $K_2CO_3$ / MeCN, ii, TsCl / NaOH / THF / $H_2O$) from catechol and 2-(2-(2-chloroethoxy)ethoxy)ethanol and was then subsequently reacted with ethyleneglycol in the presence of NaH in dry THF to afford B24C8 in a 33 % yield.
15. DB24C8 (**3**) was purchased from the Aldrich Chemical Company and used as received.
16. Brown, G. R.; Foubister, A. J. *J. Med. Chem*. **1983**, *26*, 590–592.
17. Mertens, I. J. A.; Wegh, R.; Jenneskens, L. W.; Vlietstra, E. J.; van der Kerk-van Hoof, A.; Zwikker, J. W.; Cleij, T. J.; Smeets, W. J. J.; Veldman, N.; Spek, A. L. *J. Chem. Soc., Perkin Trans. 2* **1998**, 725–735.

18. Crown ether **6** was prepared in the Bartsch group as follows: cyclization of 1,3-(*o*-hydroxyphenoxy)propane with pentaethyleneglycol dimesylate and $Cs_2CO_3$ in refluxing MeCN afforded **6** in a 53 % yield.

19. TB24C8 (**4**) is poorly soluble in MeCN, but is sufficiently soluble in $Me_2CO$ to permit such an analysis.

20. Previously (see ref. 9d), mass spectrometric analysis of an equimolar mixture of DB24C8 and bis(4-*tert*-butylbenzyl)ammonium hexafluorophosphate revealed the base peak in the spectrum to be that corresponding to the uncomplexed ammonium compound (*m/z* = 310). However, a signal arising from the 1:1 complex formed between these two components was observed at *m/z* = 758, with a relative intensity of 6 %. The significance of this result lies in the fact that the bis(4-*tert*-butylbenzyl)ammonium cation is too large to thread through the cavity of DB24C8. This restriction means that any association of these two components must occur with a *face-to-face* geometry. Even the weakest signal arising from a complex in the whole of this study, namely the peak arising from the 1:1 complex $[\mathbf{5}\cdot\mathbf{7}\text{-H}]^+$ (*m/z* = 646) has an intensity corresponding to 50 % of that observed for $\mathbf{7}^+$ (the base peak), implying that there is an interaction more enduring than a simple *face-to-face* association, *i.e.*, the threading of the cation through the macroring of DB24C8, resulting in the formation of a [2]pseudorotaxane in the gas phase.

21. In a slowly equilibrating complexation/decomplexation scenario, $K_a$ values are determined as follows: integration of the peaks in the $^1$H NMR spectrum associated with (1) free host, (2) free guest, and (3) 1:1 complex are measured, and by knowing accurately the concentrations of host and guest species that were dissolved initially, equilibrium concentrations can be determined. The $K_a$ value is then given simply by dividing the equilibrium concentration of the 1:1 complex by the product of the equilibrium concentrations of the free host and guest species. To minimize errors in this study, numerous probe protons—associated with each of the three species present in solution—were used to calculate $K_a$ values in any one spectrum. These $K_a$ values were simply averaged for each spectrum. Furthermore, at least three independent $^1$H NMR spectroscopic analyses were performed for each host:guest system, and the subsequent $K_a$ values were—once again—averaged. For leading references on this method, see Adrian, J. C.; Wilcox, C. S. *J. Am. Chem. Soc*. **1991**, *113*, 678–680.

22. The $\Delta\delta$ value combined with the distinctive coupling pattern for the $NH_2^+$-adjacent $CH_2$ protons of complexed dibenzylammonium ions is usually a good indication (ref. 8) that complexation is indeed occurring. Additionally, these spectroscopic features are also noted for molecules (rotaxanes) in which the crown ether is trapped permanently around the $NH_2^+$ center. For many examples, see ref. 9.

23. Values of $K_a$ for the 1:1 complex formed between DB24C8 (**3**) and $\mathbf{7}\cdot PF_6$ have been determined previously (see ref. 8b) in both $CD_3CN$ and $CD_3COCD_3$. The values obtained did not differ significantly and, therefore, approximate comparisons can be made between these solvents. Accordingly, the apparent lack of dibenzylammonium ion binding observed for TB24C8 is unlikely

to arise as a consequence of using $CD_3COCD_3$ instead of $CD_3CN$; rather it can most likely be attributed to an inherent property of the crown ether.

24. For leading references, see: (a) Connors, K. A. *Binding Constants*; Wiley: New York, 1987. (b) Tsukube, H.; Furuta, H.; Odani, A.; Takeda, Y.; Kudo, Y.; Inoue, Y.; Liu, Y.; Sakamoto, H.; Kimura, K. in *Comprehensive Supramolecular Chemistry, Vol. 8*; Atwood, J. L.; Davies, J. E. D.; MacNicol, D. D.; Vögtle, F.; Ripmeester, J. A., Eds.; Pergamon: Oxford, 1996; pp. 425–482 and references therein. (c) Fielding, L. *Tetrahedron* **2000**, *56*, 6151–6170.

25. The $K_a$ values calculated for hosts **2** and **3** are essentially the same within experimental error. An error of *ca*. 15 % is estimated for the calculated $K_a$ values in Table 2.2, the major source of the error originating from inaccuracies in the integrations of the appropriate $^1$H NMR signals. Although there is little difference in complexation strengths between [24]crown-8 hosts incorporating one and two benzo units, as in **2** and **3**, respectively, once all eight oxygen atoms 'become' phenolic in nature, *i.e.*, as in host **4**, the affinity of the [24]crown-8 framework for secondary dibenzylammonium ions becomes effectively zero.

26. Cantrill, S. J.; Pease, A. R.; Stoddart, J. F. *J. Chem. Soc., Dalton Trans.* **2000**, 3715–3734.

27. The X-ray crystal structure of [**3**·**8**]$PF_6$ has been reported previously, see ref. 12.

28. Whereas the term 'conformation' refers to the spatial arrangement of atoms in a single molecule—resulting from torsions about single or partial double bonds—the term 'co-conformation' describes the relative three-dimensional dispositions of (a) the constituent parts (*e.g.*, host and guest) in supramolecular systems, and of (b) the components of interlocked molecular compounds, such as catenanes and rotaxanes. See: Fyfe, M. C. T.; Glink, P. T.; Menzer, S.; Stoddart, J. F.; White, A. J. P.; Williams, D. J. *Angew. Chem., Int. Ed. Engl.* **1997**, *36*, 2068–2070.

29. For reports of C–H···F hydrogen bonding interactions, see: (a) Teff, D. J.; Huffman, J. C.; Caulton, K. G. *Inorg. Chem*. **1997**, *36*, 4372–4380. (b) Thalladi, V. R.; Weiss, H.-C.; Bläser, D.; Boese, R.; Nangia, A.; Desiraju, G. R. *J. Am. Chem. Soc*. **1998**, *120*, 8702–8710. (c) Steiner, T. *Acta Crystallogr*. **1998**, *B54*, 456–463. (d) Grepioni, F.; Cojazzi, G.; Draper, S. M.; Scully, N.; Braga, D. *Organometallics* **1998**, *17*, 296–307. (e) Dai, C.; Nguyen, P.; Marder, T. B.; Scott, A. J.; Clegg, W.; Viney, C. *Chem. Commun*. **1999**, 2493–2494. (f) Renak, M. L.; Bartholomew, G. P.; Wang, S.; Ricatto, P. J.; Lachicotte, R. J.; Bazan, G. C. *J. Am. Chem. Soc*. **1999**, *121*, 7787–7799.

30. In the realm of crown ether/dialkylammonium ion binding, the $PF_6^-$ anion-assisted formation—in the solid state—of *discrete supermolecules* with pseudorotaxane geometries, which are also stabilized by complementary C–H···F hydrogen bonding interactions, has been observed previously. See ref. 10c, and: (a) Ashton, P. R.; Fyfe, M. C. T.; Glink, P. T.; Menzer, S.; Stoddart, J. F.; White, A. J. P.; Williams, D. J. *J. Am. Chem. Soc*. **1997**, *119*, 12514–12524. (b) Ashton, P. R.; Fyfe, M. C. T.; Martínez-Díaz, M.-V.; Menzer, S.; Schiavo, C.; Stoddart, J. F.; White, A. J. P.; Williams, D. J. *Chem. Eur. J*. **1998**, *4*, 1523–1534. (c) Fyfe, M. C. T.; Stoddart, J. F.; Williams, D. J. *Struct. Chem*. **1999**, *10*, 243–259.

31. For another example of $PF_6^-$ anion encapsulation, see: McMorran, D. A.; Steel, P. J. *Angew. Chem., Int. Ed.* **1998**, *37*, 3295–3297.

32. For other solid-state examples of crown ether/acetonitrile complexes. see: (a) Allwood, B. L.; Fuller, S. E.; Ning, P. C. Y. K.; Slawin, A. M. Z.; Stoddart, J. F.; Williams, D. J. *J. Chem. Soc., Chem. Commun.* **1984**, 1356–1360. (b) Rogers, R. D.; Richards, P. D.; Voss, E. J. *J. Incl. Phenom.* **1988**, *6*, 65–71. (c) Garrell, R. L.; Smyth, J. C.; Fronczek, F. R.; Gandour, R. D. *J. Incl. Phenom.* **1988**, *6*, 73–78. (d) Rogers, R. D. *J. Incl. Phenom.* **1988**, *6*, 629–645. (e) Thuéry, P.; Nierlich, M.; Bryan, J. C.; Lamare, V.; Dozol, J.-F.; Asfari, Z.; Vicens, J. *J. Chem. Soc., Dalton Trans*. **1997**, 4191–4202.

33. After these X-ray crystallographic investigations had been completed, reports of the solid-state structures of TB24C8 (see: Bryan, J. C.; Bunick, G. J.; Sachleben, R. A. *Acta Crystallogr*. **1999**, *C55*, 250–252) and TB24C8·2MeCN (see: Bryan, J. C.; Sachleben, R. A.; Hay, B. P. *Inorg. Chim. Acta* **1999**, *290*, 86–94) also appeared in the literature. The structure factors are—within experimental error—the same. In the case of the free TB24C8 structure, the authors comment that: "*Despite the large number of arene rings in this compound, no π stacking is observed. However, close C–H···π contacts, some of which may represent hydrogen bonds are clearly present. These weak hydrogen bonds may also play a role in determining the observed crown conformation.*" This Chapter presents an analysis of these two solid-state superstructures in the context of these extensive C–H···$\pi$ networks that permeate throughout the crystalline lattices, highlighting, in particular, the dominant role that these weak intermolecular forces play in engineering the overall three-dimensional superstructures.

34. For a general consideration of the C–H···$\pi$ interaction, see: (a) Nishio, M.; Hirota, M. *Tetrahedron*, **1989**, *45*, 7201–7245. (b) Hunter, C. A. *Chem. Soc. Rev*. **1994**, 101–109. (c) Nishio, M.; Umezawa, Y.; Hirota, M.; Takeuchi, Y. *Tetrahedron* **1995**, *51*, 8665–8701. (d) Laxmi Madhavi, N. N.; Katz, A. K.; Carrell, H. L.; Nangia, A.; Desiraju, G. R. *Chem. Commun*. **1997**, 1953–1954. (e) Desiraju, G. R.; Steiner, T. *The Weak Hydrogen Bond in Structural Chemistry and Biology*; Oxford University Press: Oxford, 1999. (f) Umezawa, Y.; Tsuboyama, S.; Takahashi, H.; Uzawa, J.; Nishio, M. *Tetrahedron* **1999**, *55*, 10047–10056. Additionally, for a comprehensive list of references on almost every aspect of the C–H···$\pi$ interaction, consult the homepage of Professor Motohiro Nishio on the Internet at http://www.tim.hi-ho.ne.jp.dionisio.

35. For literature on C–H···$\pi$(aryl) hydrogen bonds, see: (a) Desiraju, G. R.; Gavezzotti, A. *J. Chem. Soc., Chem. Commun*. **1989**, 621–623. (b) Oki, M. *Acc. Chem. Res*. **1990**, *23*, 351–356. (c) Etter, M. C. *J. Phys. Chem*. **1991**, *95*, 4601–4610. (d) Zaworotko, M. J. *Chem. Soc. Rev*. **1994**, *23*, 283–288. (e) Ashton, P. R.; Preece, J. A.; Stoddart, J. F.; Tolley, M. S.; White, A. J. P.; Williams, D. J. *Synthesis* **1994**, 1344–1352. (f) Boyd, D. R.; Evans, T. A.; Jennings, W. B.; Malone, J. F.; O'Sullivan, W.; Smith, A. *Chem. Commun*. **1996**, 2269–2270. (g) Ashton, P. R.; Hörner, B.; Kocian, O.; Menzer, S.; White, A. J. P.; Stoddart, J. F.; Williams, D. J. *Synthesis* **1996**, 930–940.

36. For literature on C–H···$\pi$(alkynyl) hydrogen bonds, see: (a) Steiner, T. *Chem. Commun*. **1995**, 95–96. (b) Steiner, T.; Starikov, E. B.; Amado, A. M.; Teixeira-Dias, J. J. C. *J. Chem. Soc., Perkin Trans. 2* **1995**, 1321–1326. (c) Steiner, T.; Tamm, M.; Grzegorzewski, A.; Schulte, N.; Veldman, N.; Schreurs, A. M. M.; Kanters, J. A.; Kroon, J.; van der Maas, J.; Lutz, B. *J. Chem. Soc., Perkin Trans. 2* **1996**, 2441–2446. (d) Robinson, J. M. A.; Kariuki, B. M.; Gough, R. J.; Harris, K. D. M.; Philp, D. *J. Solid State Chem*. **1997**, *134*, 203–206. (e) Weiss, H.-C.; Bläser, D.; Boese, R.; Doughan, B. M.; Haley, M. M. *Chem. Commun*. **1997**, 1703–1704. (f) Philp, D.; Robinson, J. M. A. *J. Chem. Soc., Perkin Trans. 2* **1998**, 1643–1650. (g) Robinson, J. M. A.; Kariuki, B. M.; Harris, K. D. M.; Philp, D. *J. Chem. Soc., Perkin Trans. 2* **1998**, 2459–2469.

37. For a report of a C–H···$\pi$(alkenyl) hydrogen bond, see: Müller, T. E.; Mingos, D. M. P.; Williams, D. J. *J. Chem. Soc*., *Chem. Commun*. **1994**, 1787–1788.

38. Makriyannis, A.; Fesik, S. *J. Am. Chem. Soc*. **1982**, *104*, 6462–6463.

39. Hunter, C. A.; Sanders, J. K. M. *J. Am. Chem. Soc.* **1990**, *112*, 5525–5534.

40. Recently, the ability of other crown ethers—some not possessing [24]- or [25]crown-8 constitutions—to bind dialkylammonium ions in a 1:1 stoichiometry has been reported, see: (a) Ishow, E.; Credi, A.; Balzani, V.; Spadola, F.; Mandolini, L. *Chem. Eur. J*. **1999**, *5*, 984–989. (b) Bryant, W. S.; Guzei, I. A.; Rheingold, A. L.; Merola, J. S.; Gibson, H. W. *J. Org. Chem*. **1998**, *63*, 7634–7639. (c) Yuya, T.; Kihara, N.; Ohga, Y.; Takata, T. *Chem. Lett*. **2000**, 806–807. (d) Cantrill, S. J.; Fyfe, M. C. T.; Heiss, A. M.; Stoddart, J. F.; White, A. J. P.; Williams, D. J. *Chem. Commun*. **1999**, 1251–1252. (e) Cantrill, S. J.; Fyfe, M. C. T.; Heiss, A. M.; Stoddart, J. F.; White, A. J. P.; Williams, D. J. *Org. Lett*. **2000**, *2*, 61–64. (f) Chang, T.; Heiss, A. M.; Cantrill, S. J.; Fyfe, M. C. T.; Pease, A. R.; Rowan, S. J.; Stoddart, J. F.; White, A. J. P.; Williams, D. J. *Org. Lett*. **2000**, *2*, 2947–2950.

41. Etter, M. C. *Acc. Chem. Res*. **1990**, *23*, 120–131.

42. Jorgensen, W. L.; Severance, D. L. *J. Am. Chem. Soc*. **1990**, *112*, 4768–4774.

43. Umezawa, Y.; Tsuboyama, S.; Honda, K.; Uzawa, J.; Nishio, M. *Bull. Chem. Soc. Jpn.* **1998**, *71*, 1207–1213.

44. In a positively cooperative process, the small, but favorable, equilibrium of nucleation is overcome by the numerous favorable associations of the subsequent growth. Thus, additional interactions become a thermodynamically favored process wherein they are distinct from isodemic processes in which they have the same probability of forming as previous and subsequent interactions. For a full discussion, see: Lindsey, J. S. *New J. Chem.* **1991**, *15*, 153–180.

45. (a) Chakrabarti, P.; Samanta, U. *J. Mol. Biol*. **1995**, *251*, 9–14. (b) Maeda, I.; Shimohigashi, Y.; Ikesue, K.; Nose, T.; Ide, Y.; Kawano, K.; Ohno, M. *J. Biochem*. **1996**, *119*, 870–877. (c) Umezawa, Y.; Nishio, M. *Bioorg. Med. Chem*. **1998**, *6*, 493–504. (d) Umezawa, Y.; Nishio, M. *Bioorg. Med. Chem*. **1998**, *6*, 2507–2515. (e) Glusker, J. P. *Top. Curr. Chem*. **1998**, *198*, 1–56. (f) Umezawa, Y.; Tsuboyama, S.; Takahashi, H.; Uzawa, J.; Nishio, M. *Bioorg. Med. Chem*. **1999**, *7*, 2021–2026.

46. Perrin, D. D.; Armarego, W. F. L. *Purification of Laboratory Chemicals*; Pergamon: Oxford, 1989.
47. SHELXTL PC version 5.03, Siemens Analytical X-Ray Instruments, Inc., Madison, WI, 1994.
48. Copies of the crystallographic data can be obtained free of charge on application to CCDC, 12 Union Road, Cambridge CB12 1EZ, UK (Fax: (+44) 1223-336033; E-mail: teched@ccdc.cam. ac.uk).